Histone chaperone HIRA regulates neural progenitor cell proliferation and neurogenesis via β-catenin

Yanxin Li[1,2] and Jianwei Jiao[1,2]

[1]State Key Laboratory of Stem Cell and Reproductive Biology, Institute of Zoology, Chinese Academy of Sciences, Beijing 100101, China
[2]University of Chinese Academy of Sciences, Beijing 100049, China

Histone cell cycle regulator (HIRA) is a histone chaperone and has been identified as an epigenetic regulator. Subsequent studies have provided evidence that HIRA plays key roles in embryonic development, but its function during early neurogenesis remains unknown. Here, we demonstrate that HIRA is enriched in neural progenitor cells, and HIRA knockdown reduces neural progenitor cell proliferation, increases terminal mitosis and cell cycle exit, and ultimately results in premature neuronal differentiation. Additionally, we demonstrate that HIRA enhances β-catenin expression by recruiting H3K4 trimethyltransferase Setd1A, which increases H3K4me3 levels and heightens the promoter activity of β-catenin. Significantly, overexpression of HIRA, HIRA N-terminal domain, or β-catenin can override neurogenesis abnormities caused by HIRA defects. Collectively, these data implicate that HIRA, cooperating with Setd1A, modulates β-catenin expression and then regulates neurogenesis. This finding represents a novel epigenetic mechanism underlying the histone code and has profound and lasting implications for diseases and neurobiology.

Introduction

The mammalian cerebral cortex plays crucial roles in the formation of learning, memory, and cognition. The neurons in the neocortex are derived from multiple progenitor populations (McConnell, 1995). Among them, radial glial cells, which are the primary progenitors, produce self-renewing cells and simultaneously undergo asymmetric divisions to give rise to postmitotic neurons (Jiang and Nardelli, 2016). The normal function of the cerebral cortex is dependent on the process of neuronal production, which is often referred to as neurogenesis. During neurogenesis, the timing of self-renewal, differentiation, and maturation needs to be accurately controlled (Xu et al., 2014). The highly regulated process is orchestrated by various intracellular mechanisms and extracellular signals. Epigenetics is generally considered as a heritable change in gene expression that is not caused by alterations in the DNA sequence, and its regulation depends on the interaction between the environment and genes (Bird, 2007). Recently, it has been reported that epigenetic regulations, such as DNA and histone modifications, are involved in the highly regulated periods of neurogenesis (Yao et al., 2016). Although new light has been shed on the functions of epigenetic regulation in neurogenesis, how epigenetic molecules specifically modulate brain development still needs to be further investigated.

Histone cell cycle regulator (HIRA) is a histone chaperone and the homologue of *Saccharomyces cerevisiae* Hir1p and Hir2p. When HIRA is knocked out, many basic cellular processes are affected, resulting in DNA damage, limited de novo methylation, and aberrant transcription (Nashun et al., 2015). It is noteworthy that homozygous HIRA mutant embryos are always lethal by embryonic day 11 (E11), suggesting its important role in embryonic development. HIRA is involved in many biological processes, including gastrulation, angiogenesis, and transcriptional regulation (Dutta et al., 2010; Szenker et al., 2012; Majumder et al., 2015). DiGeorge syndrome (DGS), also called 22q11.2 deletion syndrome (McDonald-McGinn and Sullivan, 2011), is a genetic disease with cognitive impairments and learning disabilities (Zinkstok and van Amelsvoort, 2005). Several previous studies have reported that HIRA is a DGS candidate gene that maps to the DGS-specific region at 22q11 (Lorain et al., 1996; Farrell et al., 1999). Intriguingly, several studies have provided evidence that DGS patients have an ∼20-fold increased risk of schizophrenia (Bassett et al., 2003). Schizophrenia is a grievous brain disorder, and growing evidence indicates that schizophrenia is associated with neurodevelopmental defects (Ross et al., 2006; Mao et al., 2009). These findings propose the possibility that HIRA may be associated with early neural development. However, the detailed mechanisms and its role in neural progenitor cells (NPCs) remain to be defined.

β-Catenin is highly expressed in NPCs in the ventricular zone/subventricular zone (VZ/SVZ) of the cerebral cortex. It has been reported as a crucial element of the canonical Wnt signaling pathway. During neurogenesis, β-catenin plays key

Correspondence to Jianwei Jiao: jwjiao@ioz.ac.cn

Abbreviations used: ChIP, chromatin immunoprecipitation; CP, cortical plate; DGS, DiGeorge syndrome; E, embryonic day; HIRA, histone cell cycle regulator; IUE, in utero electroporation; NPC, neural progenitor cell; P, postnatal day; VZ/SVZ, ventricular zone/subventricular zone; WT, wild type.

The Rockefeller University Press $30.00
J. Cell Biol. Vol. 216 No. 7 1975–1992
https://doi.org/10.1083/jcb.201610014

roles in regulating the developmental program and can direct progenitors to proliferate or differentiate (Zechner et al., 2003).

The fundamental building block of chromatin is the nucleosome, which is composed of ∼146 bp of DNA and octamers of histone proteins. The loose packaging state is associated with active and increased gene expression, whereas compact packaging is associated with decreased gene expression. DNA methylation and chemical modification of the histone proteins determine the chromatin structure and impact gene expression (Felsenfeld and Groudine, 2003). The vast majority of functional histone modifications reside at the N-terminal tails, which protrude from the nucleosome. A variety of covalent modifications such as methylation, acetylation, ubiquitination, and phosphorylation are involved. These modifications are correlated with specific states of transcription (Fischle et al., 2003). Among them, the trimethylation of histone 3 at lysine 4 (H3K4me3) is abundant at the transcriptional start sites of genes and widely correlates with active transcription within the scope of the whole genome (Bernstein et al., 2005; Berger, 2007). However, the role of epigenetic mechanisms in brain development needs to be further elucidated.

In this study, we determine that HIRA is highly enriched in neural progenitors and that HIRA defects lead to reduced proliferation in NPCs and result in an increased proportion of cells that differentiate into neurons. Mechanically, HIRA regulates β-catenin levels by recruiting H3K4 trimethyltransferaseSetd1A and affects the level of H3K4me3, which is enriched at active transcription promoters. Additionally, we further narrowed down the functional domain of HIRA and found that the proliferation defects caused by HIRA knockdown could be rescued by overexpression of full-length HIRA, the functional domain of HIRA, or β-catenin. Collectively, our data provide firm evidence that HIRA, an epigenetic-associated molecule, plays an important role in β-catenin signaling and modulates NPC proliferation and differentiation.

Results

HIRA is expressed in the embryonic cerebral cortex and NPCs

To analyze the expression pattern of HIRA during cortical development, we obtained cerebral tissues from E13, E15, and E18 and performed Western blot. Our results showed that the expression of HIRA peaked at E15 and gradually declined as the process of development progressed (Fig. 1, A and B). Moreover, we determined that the expression of PAX6 (one type of NPC marker) was reduced as development proceeded. In contrast, the up-regulation of TUJ1 (the neuronal marker β-III-tubulin) expression was observed (Fig. 1, A, C, and D). The data suggest that HIRA may be required for embryonic cortical development. To confirm the expression patterns in vivo, E13 and E15 brain sections were collected. By immunostaining for HIRA and NESTIN, we found that HIRA protein can colocalize with NESTIN-positive NPCs residing in the VZ/SVZ of embryonic cerebral cortex at E13 and E15 (Fig. 1 E). In addition, in vitro immunofluorescence colocalization analysis showed that HIRA was coexpressed with PAX6, NESTIN, and SOX2 in cultured NPCs that were derived from E12.5 mouse brains and cultured for 48 h in proliferation medium (Fig. 1 F). For further study, we constructed two shRNA HIRA-targeting plasmids and an overexpression vector to silence or increase HIRA expression in NPCs, and the knockdown or overexpression efficiency was subsequently examined using Western blot (Fig. 1, G–J). HIRA knockdown was also confirmed by real-time PCR analysis in NPCs and N2A cells that were infected with the shRNA lentivirus (Fig. S1 A) or transfected with the shRNA plasmids (Fig. S1 B). Collectively, all these data suggest HIRA may have a potential role in regulating NPCs during the embryonic cortical development.

HIRA regulates the distribution and proliferation of NPCs

Based on the expression pattern HIRA in NPCs, we gained insight into a potential role for HIRA in neurogenesis. Then, we investigated whether HIRA was involved in the regulation of NPC proliferation in vivo using in utero electroporation (IUE). HIRA shRNA or control plasmids were electroporated into E13.5 embryonic mouse brains together with a GFP expression vector, and the embryos were sacrificed at E17.5 for phenotypic analysis. The distribution of GFP-positive cells showed that HIRA knockdown caused a marked decrease of GFP-positive cells in the VZ/SVZ and a corresponding augmentation in cells within the cortical plate (CP). Additionally, GFP-positive cells in the intermediate zone were also slightly reduced after HIRA knockdown (Fig. 2, A and B). Thus, these data reveal that HIRA knockdown results in a reduction of cells from the proliferative zone.

To further analyze the difference in GFP-positive cell positioning after HIRA knockdown, BrdU was injected into pregnant mice 2 h before the collection of embryos at E17.5. We found that HIRA defects led to a substantial reduction in GFP/BrdU double-positive NPCs (Fig. 2, C–E) and the mitotic index (Fig. 2 F) in the VZ/SVZ. When the plasmids were electroporated into embryos at E15 and collected at E19, there was almost no difference in the positioning of GFP-positive cells between the control and HIRA shRNA groups, thus ruling out an effect of HIRA knockdown on cell migration (Fig. 2, G and H). Moreover, we found that HIRA loss of function had no effect on NPC apoptosis (Fig. S2 A). In addition, a scrambled control shRNA was constructed. We found that there was almost no difference in the positioning of GFP-positive cells and 2-h BrdU labeling between the scrambled control shRNA and the empty control shRNA, excluding the possibility of potential off-target effects (Fig. S2, B–E). Overall, these data from in vivo or in vitro experiments suggest HIRA is important for maintaining NPC proliferation.

HIRA knockdown promotes cell cycle exit and neuron differentiation

Based on observations that HIRA knockdown inhibits NPC proliferation and reduced the number of GFP-positive cells in the VZ/SVZ, we raise the possibility that the NPCs may differentiate into neurons in advance. To verify this hypothesis, cell cycle exit analysis was performed. Control or HIRA shRNA plasmids were electroporated into E13.5 mouse brains, and BrdU was injected at E16.5. At E17.5, the embryonic brains were collected for immunohistochemical analysis using anti-BrdU and anti-Ki67 antibodies. We found a significant increase in the index of cell cycle exit in HIRA shRNA-treated brains (Fig. 3, A and B). In addition, we analyzed additional time points such as E13.5 to E15.5, E13.5 to E18.5, and E13.5 to postnatal day 1 (P1). In these experiments, BrdU was injected 24 h before mice sacrifice, and we discovered that all these $BrdU^+/Ki67^-$ labeling

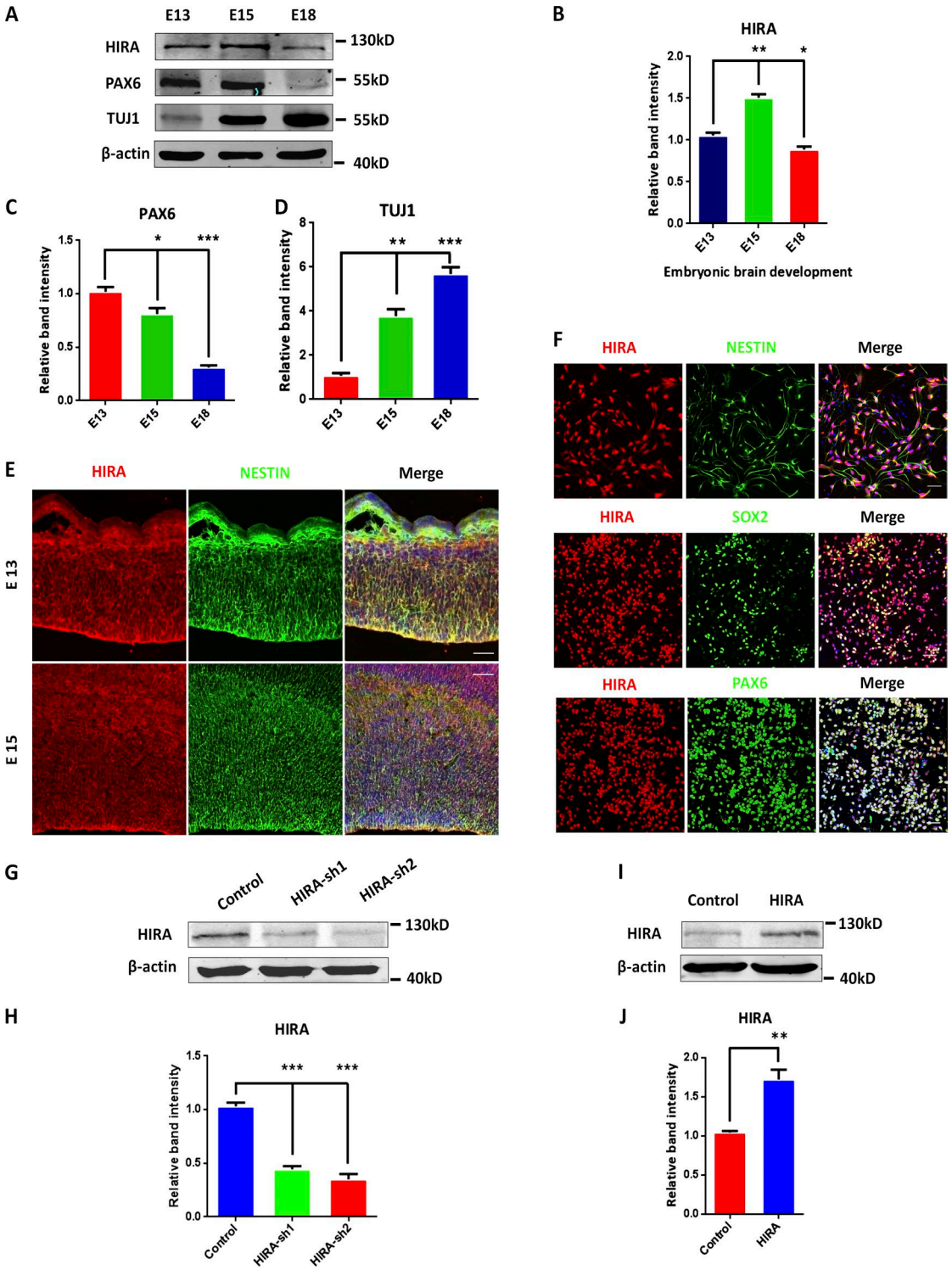

Figure 1. **HIRA is expressed in the embryonic cerebral cortex and NPCs.** (A) Western blot analysis of the protein levels of HIRA, PAX6, and TUJ1 in the mouse cerebral cortex during embryonic development. β-Actin was used as a control. (B–D) The bar graph displays the relative band intensity of HIRA (B), PAX6 (C), and TUJ1 (D) from embryonic day 13 to 18 (E13–E18; $n = 3$; mean ± SEM; *, $P < 0.05$; **, $P < 0.01$; ***, $P < 0.001$; *t* test, two sided). (E) E13 and E15 embryonic brain sections were costained with anti–HIRA and anti–NESTIN antibodies (VZ/SVZ). Bars: (E15) 25 µm; (E13) 50 µm. (F) NPCs were costained with anti–HIRA, anti–NESTIN, anti–SOX2, and anti–PAX6 antibodies. NPCs were isolated from E12.5 mouse brains and cultured in proliferation medium for 1 d. Bar, 25 µm. (G and H) In vitro–cultured NPCs were infected with control or HIRA shRNA lentivirus, and HIRA protein levels were analyzed using Western blot. The empty control shRNA was used as a control ($n = 3$; mean ± SEM; ***, $P < 0.01$; *t* test, two sided). (I and J) Western blot analysis shows the overexpression of HIRA in NPCs. The empty overexpression vector was used as a control ($n = 3$; mean ± SEM; **, $P < 0.01$; *t* test, two sided).

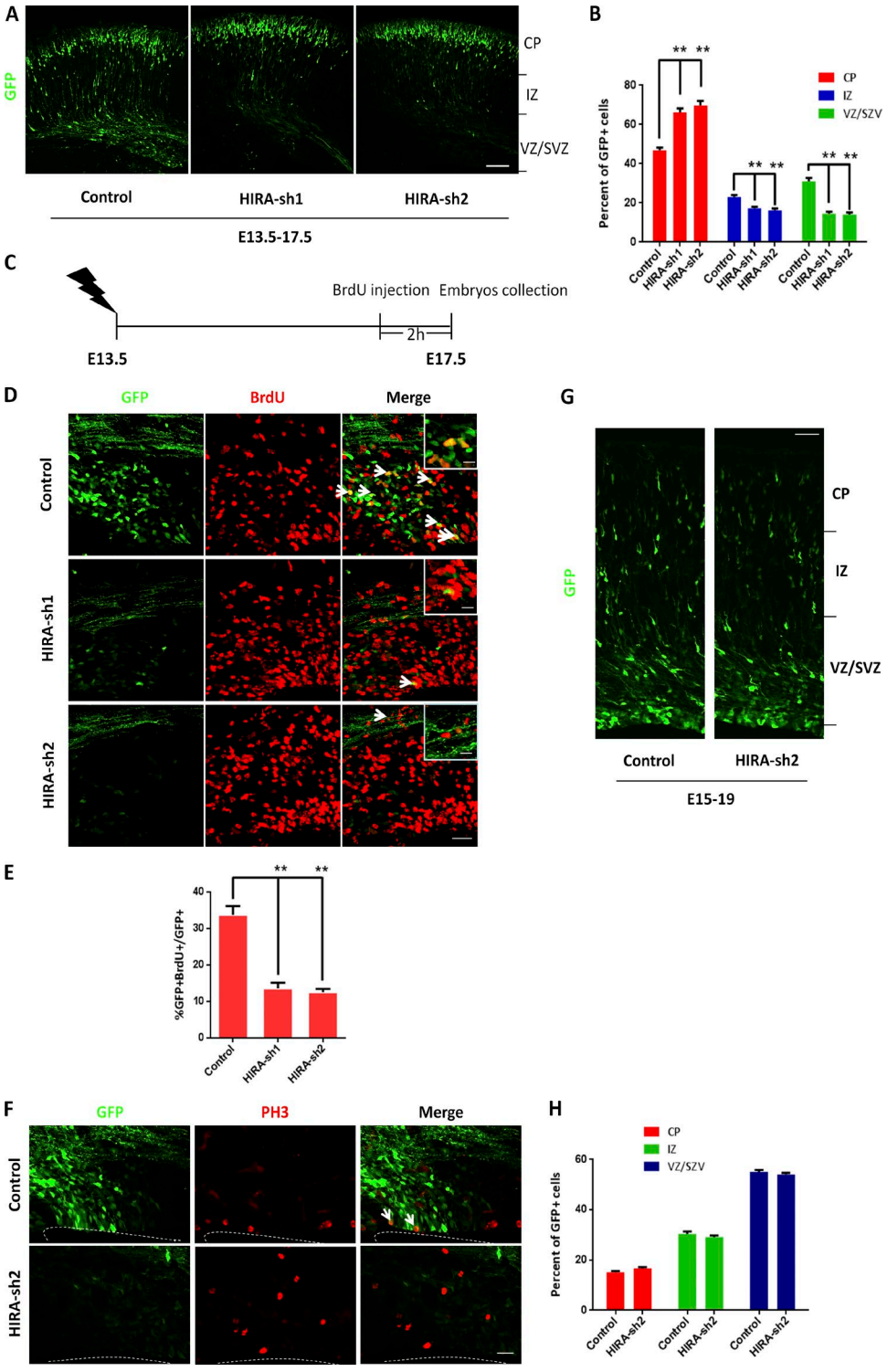

Figure 2. **HIRA regulates NPC distribution and proliferation.** (A and B) HIRA knockdown changed GFP-positive cell distribution in the cortex. HIRA shRNAs or control plasmids were electroporated into E13.5 embryonic mouse brains, and embryos were sacrificed at E17.5 for phenotypic analysis. The percentage of GFP-positive cells in each region was analyzed (n = 3; mean ± SEM; *, P < 0.05; **, P < 0.01; t test, two sided). Bar, 50 µm. CP, cortical plate; IZ, intermediate zone; VZ/SVZ, ventricular zone/subventricular zone. (C–E) BrdU and GFP double-positive cells are reduced in HIRA shRNA plasmid–electroporated brains. Brains were electroporated at E13.5, and 100 mg/kg BrdU was injected i.p. into pregnant mice 2 h before the collection of embryos at E17.5. The arrows indicate GFP/BrdU double-positive cells. Insets show high-magnification view of control and HIRA-shRNA group. The bar graph displays the percentage of GFP/BrdU double-positive cells relative to the total number of GFP-positive cells in the VZ/SVZ (n = 3; mean ± SEM; **, P < 0.01; t test, two sided). Bars: (main) 25 µm; (insets) 10 µm. (F) The mitotic index of HIRA-silenced cells is decreased in utero. The percentage of PH3 and GFP double-positive cells in the ventricular zone is shown. Arrows indicate PH3 and GFP double-positive cells. Bar, 20 µm. (G and H) HIRA knockdown has no effect on cell migration. Control or HIRA shRNA plasmids were electroporated into E15 embryonic mouse brains, and embryos were sacrificed at E19 for phenotypic analysis. The percentage of GFP-positive cells in each region is shown (n = 3; mean ± SEM; t test, two sided). Bar, 50 µm.

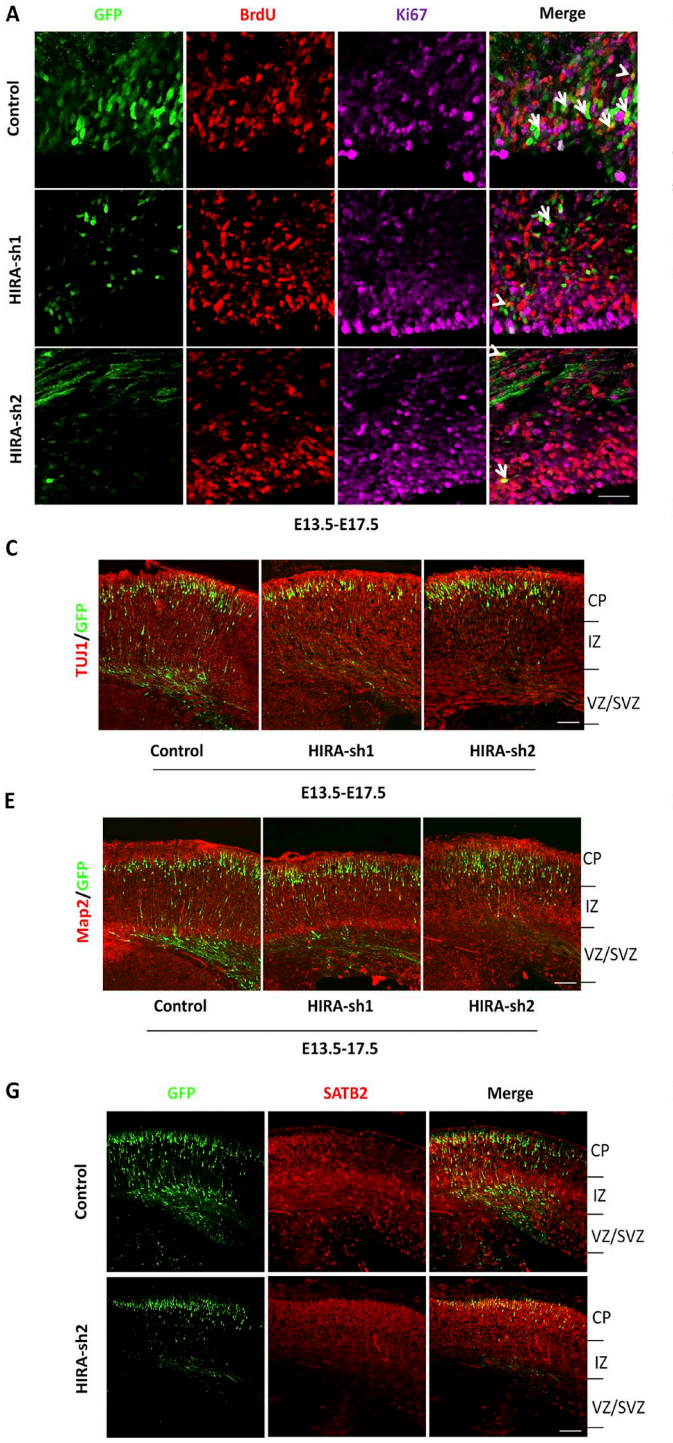

Figure 3. **HIRA loss of function facilitates cell cycle exit and neuronal differentiation.** (A and B) HIRA knockdown in NPCs increases premature cell cycle exit in utero. Control or HIRA shRNA plasmids were electroporated into E13.5 mouse brains, and BrdU was injected at E16.5. At E17.5, embryonic brains were collected for immunohistochemical analysis using anti–BrdU and anti–Ki67 antibodies. The cell cycle exit index was calculated by the percentage of GFP-positive cells that exited the cell cycle ($GFP^+BrdU^+Ki67^-$) divided by the total number of GFP and BrdU double-positive (GFP^+BrdU^+) cells. The arrows indicate $GFP^+BrdU^+Ki67^+$ cells, and the arrowheads indicate $GFP^+BrdU^+Ki67^-$ cells. The bar graph shows the percentage of $GFP^+BrdU^+Ki67^-$ cells relative to the total number of BrdU and GFP double-positive cells in the VZ/SVZ ($n = 3$; mean ± SEM; **, $P < 0.01$; *t* test, two sided). Bar, 20 µm. (C and D) HIRA knockdown increases neuronal differentiation in utero. E17.5 brain sections were stained for TUJ1 after the electroporation of control or HIRA-shRNA plasmids into the brain at E13.5. The percentage of GFP and TUJ1 double-positive cells relative to the total number of GFP-positive cells is displayed as a bar graph ($n = 3$; mean ± SEM; **, $P < 0.01$; *t* test, two sided). Bar, 50 µm. (E and F) HIRA knockdown increases neuronal differentiation in utero. E17.5 brain sections were stained for Map2 after the electroporation of control or HIRA-shRNA plasmids into the brain at E13.5. The percentage of GFP and Map2 double-positive cells relative to the total number of GFP-positive cells is displayed as a bar graph ($n = 3$; mean ± SEM; *, $P < 0.05$; **, $P < 0.01$; *t* test, two sided). Bar, 50 µm. (G and H) HIRA knockdown increases specific neuronal differentiation in utero. E17.5 brain sections were stained for SATB2 after the electroporation of control or HIRA-shRNA plasmids into the brain at E13.5. The percentage of GFP and SATB2 double-positive cells relative to the total number of GFP-positive cells is displayed as a bar graph ($n = 3$; mean ± SEM; **, $P < 0.01$; *t* test, two sided). Bar, 50 µm.

results supported that HIRA knockdown increased the number of neural progenitors exiting the cell cycle (Fig. S3, A–D).

To further investigate whether the neural progenitors exit the cell cycle and prematurely differentiate into neurons, we stained the electroporated sections with neuronal markers. The results showed an obvious increase in $TUJ1^+/GFP^+$ (Fig. 3, C and D), $Map2^+/GFP^+$ (Fig. 3, E and F), and $SATB2^+/GFP^+$ (Fig. 3, G and H) cells compared with control vector–treated brain.

Similarly, we used an in vitro culture system to evaluate the effect of HIRA on neurogenesis. The NPCs isolated from E12.5 brains were infected with either HIRA shRNA or control lentivirus. The cells were cultured in vitro for 3 d in differentiation medium. We observed an augmentation in the proportion of GFP^+TUJ1^+ cells relative to that of GFP^+ cells in the HIRA shRNA group compared with the control group (Fig. S4, A and B). Additionally, we performed the IUE experiment in vivo using wild-type HIRA (WT-HIRA) plasmid and determined that overexpression of HIRA can rescue the distribution and proliferative defects caused by HIRA knockdown (Fig. S4, C and D).

HIRA knockdown facilitates neural progenitor terminal mitosis

To investigate whether HIRA promotes the terminal mitosis of NPCs and then facilitates neuronal differentiation, we per-

formed a BrdU birthdating experiment according to a reported protocol (Duque and Rakic, 2011). As exhibited in the schematic diagram, control or HIRA shRNA plasmids were electroporated into embryonic mouse brains at E13.5, and 24 h later, BrdU was injected at E14.5. Then, the electroporated embryonic brains were collected for the analysis of terminal mitosis at E18.5 (Fig. 4 A). Because BrdU only labels cells that are in the S phase of mitosis and will be diluted with every cell cycle in continuously replicating NPCs, only the cells that are in their final mitotic division when BrdU is injected become firmly labeled and differentiate into neurons in the cortical plate. Subsequently, to detect BrdU labeling, we used an anti–BrdU antibody and observed an obvious increase in the proportion of GFP^+BrdU^+ cells relative to that of GFP^+ cells in the HIRA shRNA–treated group compared with the control group, indicating that HIRA knockdown promotes NPC terminal mitosis and thereby increases neural differentiation (Fig. 4, B and C). In addition, we extracted protein from NPCs that were cultured for 3 d after infection with either HIRA shRNA or control lentivirus and performed Western blot experiments. We determined that the expression of proliferation markers such as PAX6 and SOX2 were significantly decreased in the HIRA shRNA group. On the contrary, the expression of TUJ1 (a marker of differentiation) was markedly increased in the HIRA shRNA group compared with the control group (Fig. 4, D–F).

HIRA regulates β-catenin levels, and β-catenin rescues the HIRA knockdown–induced phenotype

To further investigate the mechanism by which HIRA influences NPC proliferation, we test the relative mRNA levels of several markers related to proliferation through RT-PCR. We found that β-catenin mRNA levels were reduced by 50% in HIRA shRNA-1–expressing cells and by 60% in HIRA shRNA-2–expressing cells, whereas the levels of other markers, such as Yap1, cyclin D1, Rest, Pax6, Sox1, Mcm2, Foxg1, and SOX2, were not obviously altered by HIRA knockdown (Fig. 5 A), suggesting that β-catenin may be associated with HIRA. On the protein level, Western blot results showed that HIRA knockdown significantly decreased β-catenin levels, which was consistent with the RT-PCR results. If HIRA is vital for β-catenin expression, one might forecast that the transcriptional targets of β-catenin may be reduced by HIRA loss of function. Axin2 (Leung et al., 2002) is a well-established β-catenin transcription target. We observed that Axin2 was decreased after HIRA knockdown (Fig. 5, B and C). We further assessed the effect of HIRA gain of function on total β-catenin levels. Conversely, the overexpression of WT-HIRA enhanced PAX6 levels, reduced TUJ1 levels, and increased total β-catenin levels in primary NPCs (Fig. 5, D and E). In the embryonic cerebral cortex, we observed that β-catenin was enriched in NESTIN-positive neural progenitors residing in the VZ/SVZ at E13 and E15 (Fig. 5 F). In cultured NPCs, β-catenin was robustly expressed in NESTIN-, SOX2-, and PAX6-positive cells (Fig. S5 A). Furthermore, we used two previously characterized shRNAs (Mao et al., 2009) that target endogenous β-catenin, and their knockdown efficiency was confirmed though Western blot analysis (Fig. 5, G and H). When transfected or infected with these shRNAs in vitro, HIRA immunostaining was decreased in both N2A cells and primary NPCs (Fig. S5, B and C). Next, using the two β-catenin shRNAs, the E13.5–17.5 IUE experiment was performed. Similarly, β-catenin knockdown changed the cell distribution in the cerebral cortex,

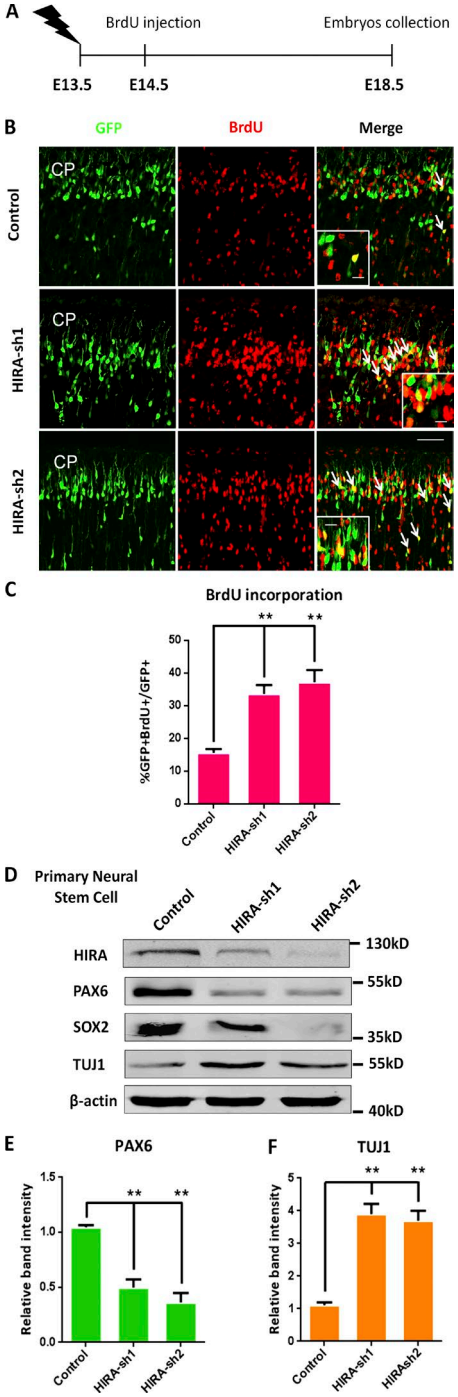

Figure 4. **HIRA knockdown promotes NPC terminal mitosis.** (A) The timeline shows the process of the BrdU birthdating experiment. (B and C) Control or HIRA shRNA plasmids were electroporated into embryonic mouse brains at E13.5, and BrdU was injected at E14.5. Then, the electroporated embryonic brains were collected for immunohistochemical analysis using an anti–BrdU antibody at E18.5. The arrows indicate BrdU and GFP double-positive cells. Insets show high-magnification views. Bars: (main) 25 µm; (insets) 10 µm for. The bar graph exhibits the percentage of GFP and BrdU double-positive cells relative to the total number of GFP-positive cells in the CP (n = 3; mean ± SEM; **, $P < 0.01$; t test, two sided). (D–F) The protein levels of PAX6, SOX2, and TUJ1 were determined by Western blot analysis in mouse NPCs after the infection of control or HIRA-shRNA lentivirus. β-actin was used as a control. The bar graphs show the relative band intensity of PAX6 (E) and TUJ1 (F) in mouse NPCs (n = 3; mean ± SEM; **, $P < 0.01$; t test, two sided).

increased the percentage of GFP-positive cells in the CP, and reduced the number of GFP-positive cells in the VZ/SVZ (Fig. 5, I and J). β-Catenin knockdown also increased the number of TUJ1$^+$/GFP$^+$ cells (Fig. 6, A and B) and facilitated neural progenitor terminal mitosis (Fig. 6, C and D), which recapitulated the phenotype of HIRA knockdown.

To decipher the relationship between HIRA and β-catenin in embryonic development, a rescue experiment was conducted. We found that β-catenin overexpression rescued the distribution and proliferative defects caused by HIRA knockdown in vivo (Fig. 6, E and F). Increased β-catenin levels rescued the TUJ1$^+$/GFP$^+$ cells caused by HIRA knockdown in primary NPCs in vitro (Fig. 6, G and H). Together, these data suggest that HIRA controls progenitor cell proliferation by modulating β-catenin levels.

HIRA N-terminal domain can rescue the change in the distribution and proliferation of NPCs caused by HIRA knockdown

To narrow down the functional domain of HIRA, we generated three Flag-tagged segments, which included 1–401 aa (N-terminal residues), 402–703 aa (middle residues), and 704–1,019 aa (C-terminal residues; Fig. 7 A). We found that the decrease in β-catenin levels caused by HIRA knockdown was rescued by the coinfection of HIRA-segment 1 into NPCs (Fig. 7, B and C). Next, to further examine the function of each segment in vivo, an IUE experiment was conducted at E13.5–E17.5. Coelectroporation of HIRA-segment 1 with HIRA-sh2 could successfully rescue the cell distribution or TUJ1$^+$/GFP$^+$ cell proportion changes caused by HIRA knockdown, but coelectroporation with HIRA-Seg2 or HIRA-Seg3 with HIRA-shRNA-2 did not appear to change the HIRA-knockdown phenotype (Fig. 7, D–G). Given that increased β-catenin levels rescue the distribution and proliferative defects caused by HIRA knockdown, we gained insight into the mechanism by which HIRA affects β-catenin levels and regulates NPC proliferation. A chromatin immunoprecipitation (ChIP) assay was performed, and the results showed that when full-length Flag-HIRA was overexpressed (samples were pulled down by the anti–Flag antibody), the amount of HIRA that bound to −0.5 kb of the β-catenin promoter was markedly increased more than fourfold, and the increase was gradually reduced as the distance away from the transcriptional start site increased. In addition, the detection of HIRA bound to the CDS of β-catenin was selected as a negative control (Fig. 7 H). Meanwhile, the binding of HIRA to other proliferative genes of PAX6 and SOX2 were examined. ChIP-qPCR results showed that overexpression of Flag-HIRA (samples were pulled down by the anti–Flag antibody) resulted in some binding to PAX6 promoter and almost no binding to the SOX2 promoter (Fig. S5 D). Obviously, the binding of HIRA to the β-catenin promoter was the strongest. To further understand the segmental function of HIRA, we conducted more ChIP assays using Flag-tagged segment 1 (Seg1), segment 2 (Seg2), and segment 3 (Seg3). The results showed that when HIRA-Seg1 was overexpressed, the amount of HIRA that bound to −0.5 kb of the β-catenin promoter was the largest compared with HIRA-Seg2 and HIRA-Seg3 (Fig. 7 I), revealing that HIRA-Seg1 possesses the most potent activity. All these results reveal that HIRA binds to the β-catenin promoter to activate its expression and that segment 1 is the functional domain of HIRA, which plays an important role in modulating the proliferation of NPCs.

Reduced H3K4me3 inhibits β-catenin expression when HIRA is knocked down

To further decipher how HIRA activates β-catenin expression, we detected the expression levels of several histone protein markers, such as H3k27me3, H3K4me3, H3k36me3, and H4k16ac, by Western blot analysis. Only H3K4me3 was significantly reduced when HIRA was knocked down, and conversely, the overexpression of HIRA increased H3K4me3 levels, suggesting that H3K4me3 is associated with HIRA (Fig. 8, A–D). Previous studies have established that histone H3 lysine 4 trimethylation (H3K4me3) is frequently regarded as a mark of actively transcribed promoters (Barski et al., 2007; Guenther et al., 2007). Thus, we predicted that reduced H3K4me3 attenuates β-catenin expression via the inhibition of transcription when HIRA is silenced. Immunofluorescence colocalization analysis revealed that H3K4me3 was colocalized with HIRA in NPCs, indicating that they may work together in regulating the β-catenin pathway (Fig. 8 E). Additionally, we performed a gradient test regarding the amount of transfected HIRA-sh2. The results showed that along with the reduction of transfected HIRA-sh2, the expression of H3K4me3 and the total β-catenin levels were gradually decreased, confirming the effect of HIRA loss of function on H3K4me3 and total β-catenin levels. The levels of proliferation markers such as PAX6, PCNA, and SOX2 were decreased, and the expression of TUJ1 was significantly increased, further proving the proliferative defect caused by HIRA knockdown (Fig. 8, F and G). Collectively, these data indicate that reduced H3K4me3 inhibits β-catenin expression by HIRA knockdown.

HIRA increases the recruitment of the H3K4 trimethyltransferase Setd1A, promotes β-catenin expression, and further enhances NPC proliferation

For further analyses, we sought out the effect of H3K4 trimethyltransferase Setd1A. Interestingly, previous studies have reported that Setd1A loss of function is associated with developmental disorders and schizophrenia (Takata et al., 2014; Singh et al., 2016). Thus, we created two shRNAs that efficiently silenced Setd1A expression (Fig. S6 A) and a Setd1A-HA vector that overexpressed Setd1A (Fig. S6 B). In vivo IUE results showed that Setd1A knockdown increased the percentage of GFP-positive cells in the CP and decreased BrdU labeling (Fig. 9, A–C; and Fig. S6 E). We also found a significant increase in the proportion of GFP$^+$TUJ1$^+$ cells relative to that of GFP$^+$ cells in Setd1A-sh2-treated brains compared with controls (Fig. S6, C and D). Additionally, we verified that Setd1A overexpression increased the expression level of H3K4me3, and conversely, when Setd1A was down-regulated, the expression level of H3K4me3 was reduced (Fig. S6 F). To determine whether HIRA works with Setd1A in modulating the proliferation of NPCs, we performed Western blot analysis. When HIRA and Setd1A lentivirus were coinfected into NPCs, the proliferative tendency was more obviously increased and the expression of TUJ1 was decreased, supporting the notion that HIRA functions together with Setd1A in regulating β-catenin–mediated proliferation (Fig. 9, D and E). To further decipher the cooperative actions of HIRA and Setd1A, we performed a co-ChIP assay. In this experiment, HIRA-Flag and Setd1A-HA lentiviruses were delivered into NPCs and ChIP was performed by anti–Flag antibody. The amount of HIRA that bound to the −0.5 kb region of the β-catenin promoter was increased in the coinfection group compared with HIRA or Setd1A alone, demonstrating that HIRA can cooperate with

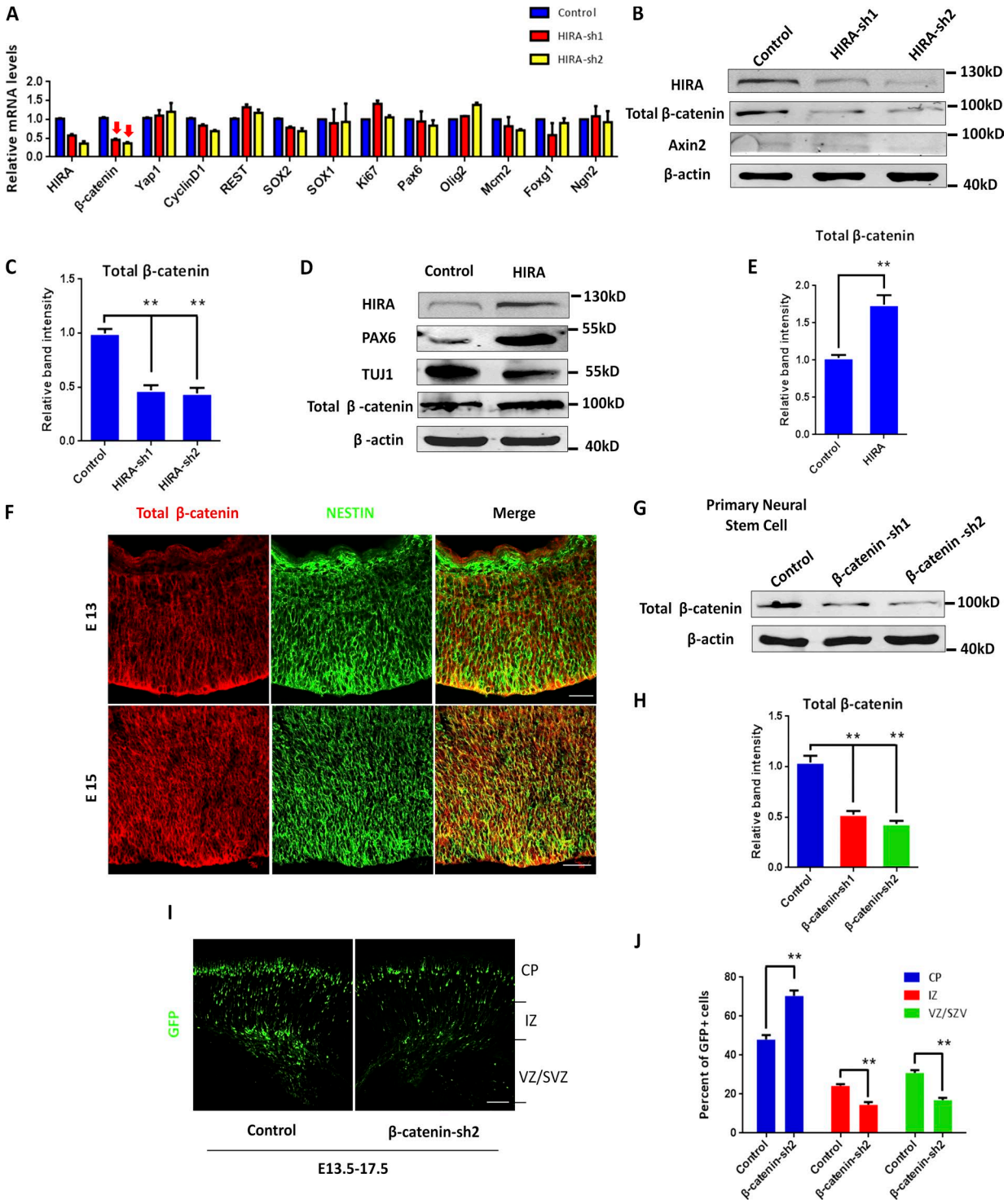

Figure 5. **HIRA regulates β-catenin levels.** (A) RT-PCR analysis of the relative mRNA levels of several markers related to proliferation and differentiation when HIRA is silenced. The arrows indicate the decrease in β-catenin expression levels when HIRA is knocked down. (B and C) Western blot analysis of the protein levels of total β-catenin and Axin2 in HIRA-silenced NPCs. The empty control shRNA was used as a control. The bar graph shows the relative band intensity of total β-catenin. β-Actin was used as a loading control (n = 3; mean ± SEM; *, P < 0.05; **, P < 0.01; t test, two sided). (D and E) Western blot analysis of the protein levels of total β-catenin, PAX6, and TUJ1 in HIRA-overexpressing NPCs. The empty control expression vector was used as a control. The bar graph shows the relative band intensity of total β-catenin. β-Actin was used as a loading control (n = 3; mean ± SEM; **, P < 0.01; t test, two sided). (F) E13 and E15 embryonic brain sections were costained with anti–β-catenin and anti–NESTIN antibodies (VZ/SVZ). Bars: (E15) 25 µm; (E13) 50 µm. (G and H) Cultured NPCs were infected with control or β-catenin shRNA lentivirus, and total β-catenin protein levels were then analyzed using Western blot. The empty control shRNA was used as a control. The bar graph shows the relative band intensity of total β-catenin. β-Actin was used as a loading control (n = 3; mean ± SEM; **, P < 0.01; t test, two sided). (I and J) β-Catenin knockdown leads to changes in GFP-positive cell distribution in the cortex. β-Catenin shRNA or control plasmids were electroporated into E13.5 embryonic mouse brains, and embryos were sacrificed at E17.5 for phenotypic analysis. The percentage of GFP-positive cells in each region is shown (n = 3; mean ± SEM; **, P < 0.01; t test, two sided). Bar, 50 µm.

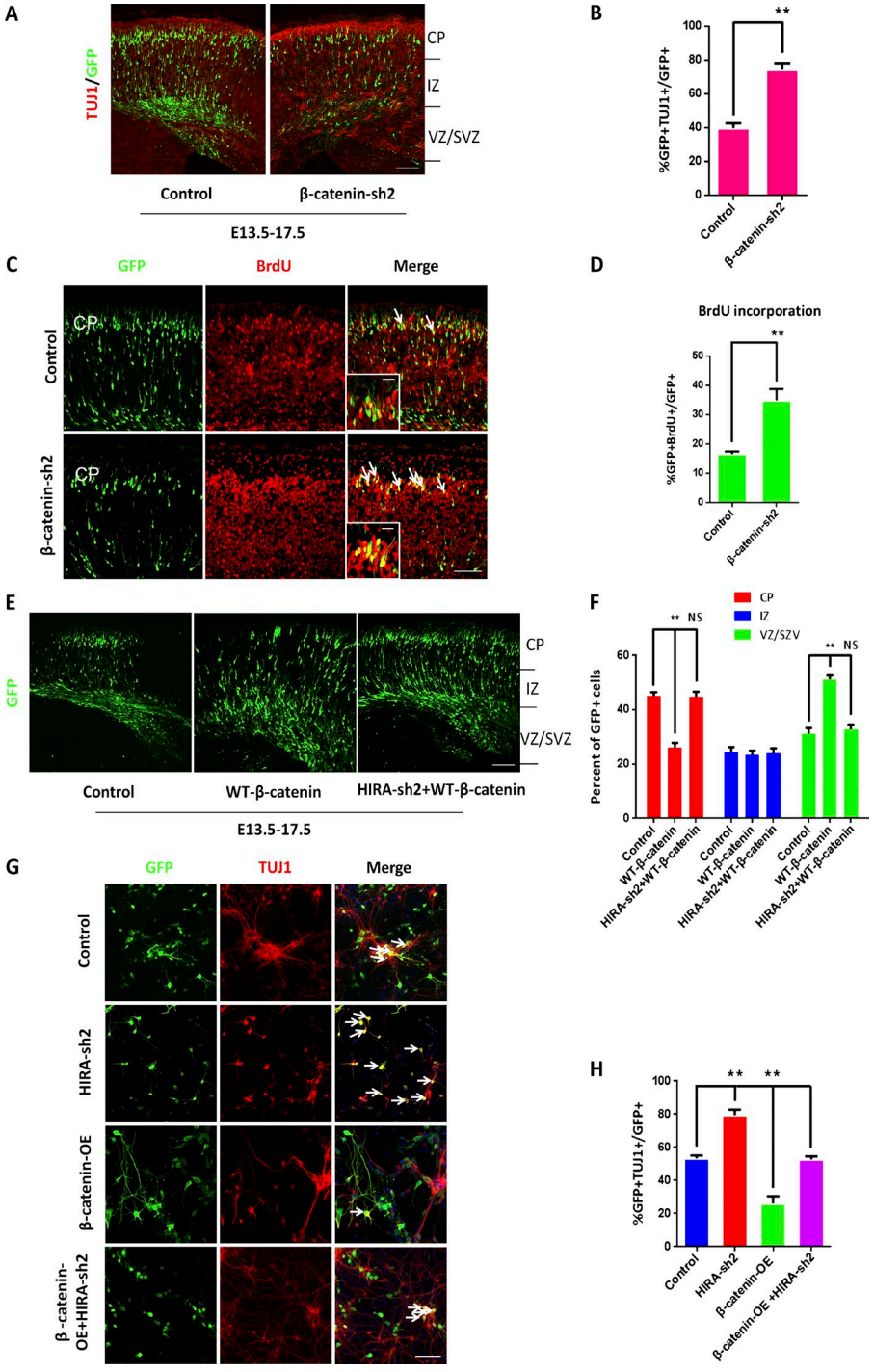

Figure 6. **Overexpression of β-catenin rescues the HIRA knockdown–induced phenotype.** (A and B) β-Catenin knockdown increases neuronal differentiation in utero. E17.5 brain sections were stained for anti–TUJ1 antibody after the electroporation of control or β-catenin shRNA plasmids into the brain at E13.5. The percentage of GFP and TUJ1 double-positive cells relative to the total number of GFP-positive cells is displayed as a bar graph (n = 3; mean ± SEM; **, P < 0.01; t test, two sided). Bar, 50 µm. (C and D) β-Catenin knockdown promotes NPC terminal mitosis. Control or β-catenin shRNA plasmids were electroporated into embryonic mouse brains at E13.5, and BrdU was injected at E14.5. Then, the electroporated embryonic brains were collected for immunohistochemical analysis using an anti–BrdU antibody at E18.5. The arrows indicate BrdU and GFP double-positive cells. Insets show high-magnification views. The bar graph shows the percentage of GFP and BrdU double-positive cells relative to the total number of GFP-positive cells in the CP (n = 3; mean ± SEM; **, P < 0.01; t test, two sided). Bars: (main) 25 µm; (insets) 10 µm. (E and F) β-Catenin rescue the positioning defects caused by HIRA knockdown in vivo. Control, WT-β-catenin, or HIRA shRNA together with WT-β-catenin plasmids were electroporated into E13.5 embryonic mouse brains, and embryos were sacrificed at E17.5 for phenotypic analysis. The percentage of GFP-positive cells in each region is exhibited (n = 3; mean ± SEM; **, P < 0.01; NS, not significant; t test, two sided). Bar, 50 µm. (G and H) β-Catenin rescues the proliferative defects caused by HIRA loss of function in vitro. NPCs were isolated from E12.5 embryonic mouse brains and cultured for 1 d. Subsequently, NPCs were infected with control, HIRA shRNA, β-catenin overexpression, or HIRA shRNA together with β-catenin overexpression lentivirus.The arrows show some GFP-positive cells. The percentage of TUJ1and GFP double-positive cells divided by the total number of GFP-positive cells is shown as a bar graph (n = 3; mean ± SEM; **, P < 0.01; t test, two sided). Bar, 25 µm.

Setd1A to enhance binding to the −0.5 kb region of the β-catenin promoter (Fig. 9 F). For a more detailed study, we additionally conducted the co-ChIP experiment using segmental HIRA. The results indicated that HIRA-Seg1 has the most noticeable effect on β-catenin promoter binding (Fig. 9 G). Meanwhile, when Setd1A-HA was overexpressed together with Flag-HIRA-Seg1, Seg2, or Seg3 and the samples were pulled down by the anti–HA antibody, the amount of Setd1A that bound to the −0.5 kb region of the β-catenin promoter was increased in the presence of HIRA-Seg1, but not HIRA-Seg2 or Seg3 (Fig. S6 I). To determine whether HIRA and Setd1A directly interact with each other, we create Flag-tagged HIRA and performed an in vitro association experiment using HA-tagged Setd1A. The coimmunoprecipitation experiment showed that HIRA and Setd1A can be immunoprecipitated together (Fig. 9, H and I). To confirm the relationship between HIRA and Setd1A, Western blot analysis was performed to detect β-catenin expression in neural progenitors. We found that Setd1A can rescue decreased β-catenin expression levels by HIRA knockdown. Further, knockdown by both HIRA and Setd1A reduced more β-catenin expression levels compared with HIRA or Setd1A alone (Fig. 10, A and B). To test which segment of HIRA physically interacts with Setd1A, we performed coimmunoprecipitation experiments using HIRA-Seg1, Seg2, or Seg3. The results showed that all

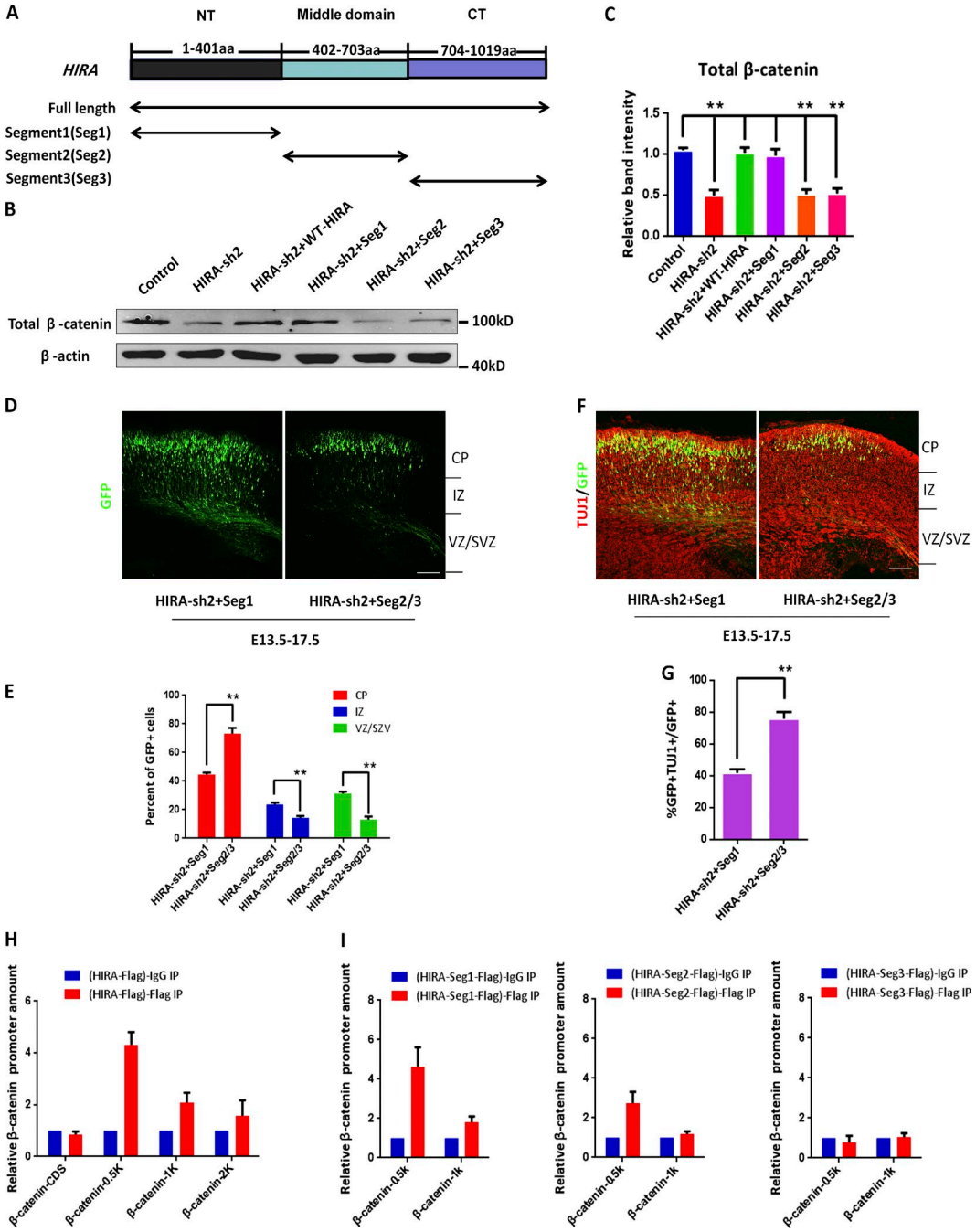

Figure 7. **HIRA N-terminal domain can rescue the changes in cell distribution and the proliferative defects caused by HIRA knockdown.** (A) The schematic diagram shows the different structural segments of HIRA. Segment 1 (Seg1, N terminal), 1–401 aa; segment 2 (Seg2, middle), 402–703 aa; and segment 3 (Seg3, C terminal), 704–1,019 aa. (B and C) HIRA segment 1 can rescue the reduced β-catenin levels caused by HIRA knockdown in neural progenitors. NPCs were isolated from E12.5 embryonic mouse brains and cultured for 24 h. Subsequently, NPCs were infected with lentiviruses of control, HIRA-sh2, HIRA-sh2 together with WT-HIRA, HIRA-sh2 together with HIRA Seg1, HIRA-sh2 together with Seg2, or HIRA-sh2 together with Seg3. The bar graph shows the Western blot analysis of total β-catenin protein levels (n = 3; mean ± SEM; **, $P < 0.01$; t test two-sided). (D and E) HIRA segment 1 can rescue the changes in NPC distribution caused by HIRA knockdown in vivo. HIRA-sh2 together with HIRA Seg1 or HIRA-sh2 together with Seg2 or Seg3 plasmids were electroporated into E13.5 embryonic mouse brains, and the embryos were sacrificed at E17.5 for phenotypic analysis. The percentage of GFP-positive cells in each region is exhibited (n = 3; mean ± SEM; *, $P < 0.05$; **, $P < 0.01$; t test, two sided). Bar, 50 µm. (F and G) HIRA segment 1 can rescue the proliferative defects caused by HIRA knockdown in utero. E17.5 brain sections were stained for TUJ1 after the electroporation of HIRA-sh2 together with Seg1 plasmids or HIRA-sh2 together with Seg2 or seg3 plasmids into the brain at E13.5. The percentage of GFP and TUJ1 double-positive cells relative to the total number of GFP-positive cells is displayed as a bar graph (n = 3; mean ± SEM; **, $P < 0.01$; t test two-sided). Bar, 50 µm. (H) HIRA regulates β-catenin levels by binding to the β-catenin promoter. Primary NPCs cultured in vitro were transfected with control or HIRA overexpression lentiviruses. The binding of HIRA to the β-catenin promoter was determined through ChIP and real-time PCR (n = 3; mean ± SEM). (I) HIRA-Seg1 modulates β-catenin expression by binding to the β-catenin promoter. Primary NPCs cultured in vitro were infected with the control, HIRA-Seg1, HIRA-Seg2, or HIRA-Seg3 overexpression lentiviruses. The binding of HIRA to the β-catenin promoter was determined through ChIP and real-time PCR (n = 3; mean ± SEM). IZ, intermediate zone.

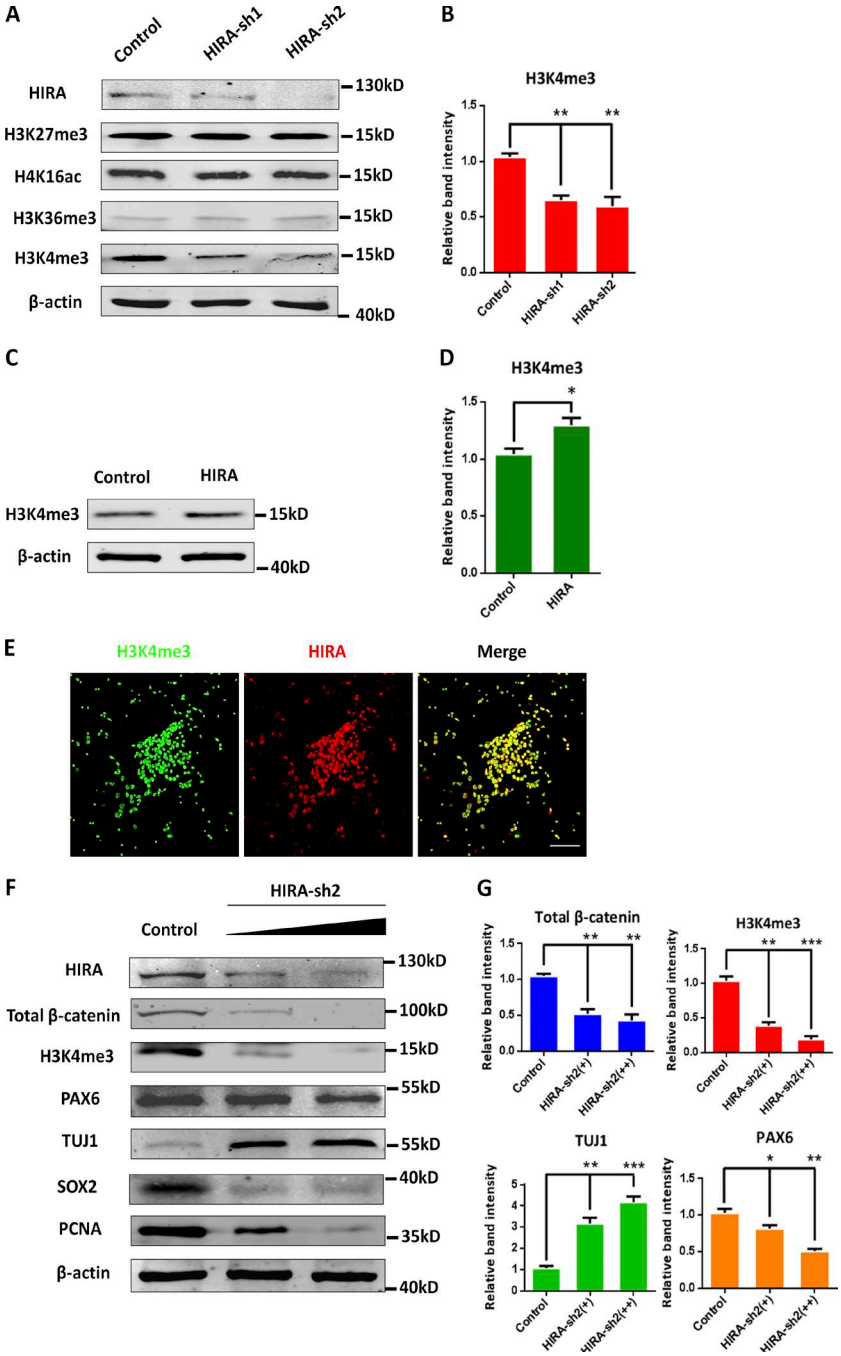

Figure 8. **HIRA knockdown reduces H3K4me3 levels.** (A and B) Expression of H3K4me3 is obviously reduced when HIRA is knocked down. Western blot analysis of the protein levels of H3k27me3, H4k16ac, H3k36me3, and H3K4me3 in HIRA-silenced NPCs. The empty control shRNA was used as a control. The bar graph shows the relative band intensity of H3K4me3. β-Actin was used as a loading control (n = 3; mean ± SEM; **, P < 0.01; t test, two sided). (C and D) Western blot analysis of the protein levels of H3K4me3 in HIRA-overexpressing NPCs. The control expression vector was used as a control. The bar graph shows the relative band intensity of H3K4me3. β-Actin was used as a loading control (n = 3; mean ± SEM; *, P < 0.05; t test, two sided). (E) H3K4me3 and HIRA colocalize in NPCs. Cultured NPCs were costained with anti–H3K4me3 and anti–HIRA antibodies. Bar, 25 µm. (F and G) Western blot analysis of the protein levels of total β-catenin, H3K4me3, PAX6, TUJ1, SOX2, and PCNA with gradually increasing transfection amounts of HIRA-sh2 (0 µg, 0.5 µg, and 1.5 µg). The bar graph shows the relative band intensity of total β-catenin, H3K4me3, TUJ1, and PAX6. β-Actin was used as a loading control (n = 3; mean ± SEM; *, P < 0.05; **, P < 0.01; ***, P < 0.001; t test, two sided).

three segments could interact with Setd1A, but seg1 has a little more interaction (Fig. 10 C). Through Western blot analysis, we found that when Setd1A was knocked down, the expression levels of PAX6, SOX2, and β-catenin were reduced (Fig. 10 D), which was consistent with the results of Setd1A knockdown in vivo. To confirm whether H3K4me3 deposition at the β-catenin locus changes upon HIRA overexpression or knockdown, we performed a ChIP-qPCR assay. The results showed that when HIRA was overexpressed and pulled down by the anti–H3K4me3 antibody, the amount of H3K4me3 that bound to −0.5 kb of the β-catenin promoter was markedly increased (more than threefold), and the increase was gradually reduced as the distance from the transcriptional start site increased. Meanwhile, when HIRA was knocked down, the amount of H3K4me3 that bound to −0.5 kb and −1 kb of the β-catenin promoter was significantly reduced (Fig. 10 E), suggesting that HIRA is involved in regulation of H3K4me3 levels. The coimmunoprecipitation results also showed that when both HIRA-Flag and Setd1A-HA were coexpressed, the amount of total β-catenin and H3K4me3 that was pulled down by HIRA-Flag was prominently increased (Fig. 10 F). By comparison, H3K4me3 showed some binding to the PAX6 promoter and almost no binding to the SOX2 promoter when the samples were pulled down by the anti–H3K4me3 antibody (Fig. S6 G). To provide mechanistic insights on the potential interaction between HIRA and β-catenin, we performed a coimmunoprecipitation assay and found that there was no interaction between HIRA and β-catenin on the protein level (Fig. S6 H). All the expression levels related to the ChIP-qPCR experiments that are in the main figures are listed in Fig. S7. Collectively, these results suggest that HIRA increases

the recruitment of the H3K4me3 trimethyltransferase Setd1A, promotes β-catenin expression, and further enhances NPC proliferation (Fig. 10 G).

Discussion

Recent studies have shown that epigenetic regulation is involved in many biological processes (Reik, 2007; Gregoire et al., 2016; Stratton and McKinsey, 2016). HIRA, a histone chaperone, has also been regarded as a DGS-associated gene (Farrell et al., 1999). Generally, DGS patients share some common characteristics, such as cognitive impairment, and have an increased risk of schizophrenia, which is often caused by defects during neurodevelopment (Bassett et al., 2003). However, there is no direct evidence that proves whether or how HIRA affects brain development. Neurogenesis is a complicated process that is heavily regulated by a diverse array of extracellular and intracellular activities and factors. Here, we demonstrate that HIRA is required for NPC proliferation and provide multiple lines of evidence indicating an essential role for HIRA in maintaining a pool of progenitor cells during embryonic brain development. Our results may provide a new understanding of epigenetic regulation, which contributes to normal brain development and disease pathophysiology.

Previous studies have shown that HIRA is widely expressed at various stages of mouse embryo (Wilming et al., 1997). We also observe that HIRA is abundant in NPCs and that its expression peaks at E15, during the period of neurogenesis (Qian et al., 2000). Thus, this finding indicates that HIRA may play an essential role during early neocortical development. Subsequent studies have shown that HIRA-mediated histone deposition is associated with neuronal plasticity and cognition in both embryonic and adult brains (Maze et al., 2015). In our study, the results suggest that HIRA is essential for normal cortical development in the embryonic brain. We find that HIRA loss of function leads to proliferation defects, including a rapid reduction of the NPC pool and an increase in the differentiation of NPCs. Our data show that HIRA knockdown increases terminal mitosis of premature NPCs and changes the neuronal morphology to a more abundant state. We also checked the cell migration by electroporating embryonic brain at E15 and collecting brain at E19 and found no difference when HIRA is knockdown. However, E15 is another initial time point for astrocyte differentiation, and more studies will be performed in the future to investigate whether HIRA affects astrocyte differentiation.

To further decipher the mechanisms underlying the phenotype caused by HIRA knockdown, we performed RT-PCR analysis and found that the expression of β-catenin was significantly reduced when HIRA was silenced. β-Catenin is a core downstream effector of the canonical Wnt signaling pathway, which plays important roles in numerous cellular activities, including cell proliferation and cell fate decisions (Niehrs, 2012; Clevers et al., 2014). It has been reported that β-catenin is involved in the regulation of NPC expansion and the maintenance of stemness in NPCs (Zechner et al., 2003). In our study, we observe that β-catenin is enriched in the VZ/SVZ and colocalizes with NESTIN, which has been identified as an NPC marker (Wiese et al., 2004). Electroporation of β-catenin shRNAs at E13–E17 tended to inhibit progenitor self-renewal, which is similar to the effect observed after HIRA knockdown. When HIRA was divided into three Flag-tagged segments, HIRA-seg1 containing the WD40 domain had an effect on NPCs similar to full-length HIRA. This is consistent with the functional description of WDR62, which has been previously reported (Xu et al., 2014).

Subsequently, we investigated the potential mechanism on the transcriptional level to illuminate how HIRA activates the expression of β-catenin. Thus, we detected changes in the expression of several histone markers when HIRA was silenced. H3K4me3 is traditionally identified as a histone marker that mainly surrounds the transcription initiation site of active genes (Shen et al., 2015a), and we observed that only the level of H3K4me3 was obviously reduced when HIRA was knocked down, raising the possibility that HIRA enhances the expression of β-catenin through increased H3K4me3 expression. ChIP analysis has been widely used to explore the interaction between DNA and protein in cells (Collas, 2010). Therefore, we performed a ChIP analysis and confirmed that HIRA could bind to the promoter of β-catenin. It has been reported that the H3K4 trimethyltransferase Setd1A participates in the regulation of cell cycle progression (Tajima et al., 2015), and its loss of function increases the risk of schizophrenia and developmental disorders (Takata et al., 2014; Singh et al., 2016). However, its role in NPCs and in schizophrenia pathogenesis remains unknown. Surprisingly, in our study, we demonstrated that Setd1A knockdown changes cell distribution and inhibits NPC proliferation, which is reminiscent of the phenotype observed after HIRA knockdown. This finding may explain the high risk of schizophrenia associated with Setd1A loss of function. Coimmunoprecipitation is a powerful experimental technique that is usually applied to analyze protein-protein interactions in many researches (Lin et al., 2016). Here, we performed coimmunoprecipitaion analysis and confirmed the interaction between HIRA and Setd1A. Meanwhile, when HIRA and Sed1A are simultaneously overexpressed, the relative amount of bound β-catenin promoter is increased. These data illustrated that HIRA and Setd1A interact with each other and can cooperatively function in modulating NPC proliferation. However, whether the mutations in H3K4me3 disturb the function of HIRA and Setd1A requires further investigation.

In summary, this study uncovers an essential role of HIRA in modulating the β-catenin pathway during neurogenesis and normal neurodevelopment. HIRA knockdown may disturb the balance between NPC proliferation and differentiation, ultimately resulting in developmental disorders. These results provide a new understanding of the novel function of epigenetic regulation in early cortical development and provide far-reaching implications for diseases and neurobiology.

Materials and methods

Animals

Pregnant ICR mice were purchased from Charles River. All animal studies were performed in accordance with standard experimental protocols, and all procedures involving mice were approved by the Care and Use of Animals Committee of the Institute of Zoology at the Chinese Academy of Sciences.

Plasmid constructs

The oligonucleotides that target HIRA, β-catenin, and Setd1A were cloned into the lentiviral vector pSicoR-GFP (Addgene). The shRNA sequences that targeted HIRA were HIRA-sh1, 5′-CCAGCTTTCCAC AGCTGTTAT-3′ (Dutta et al., 2010), and HIRA-sh2, 5′-CTCAAG

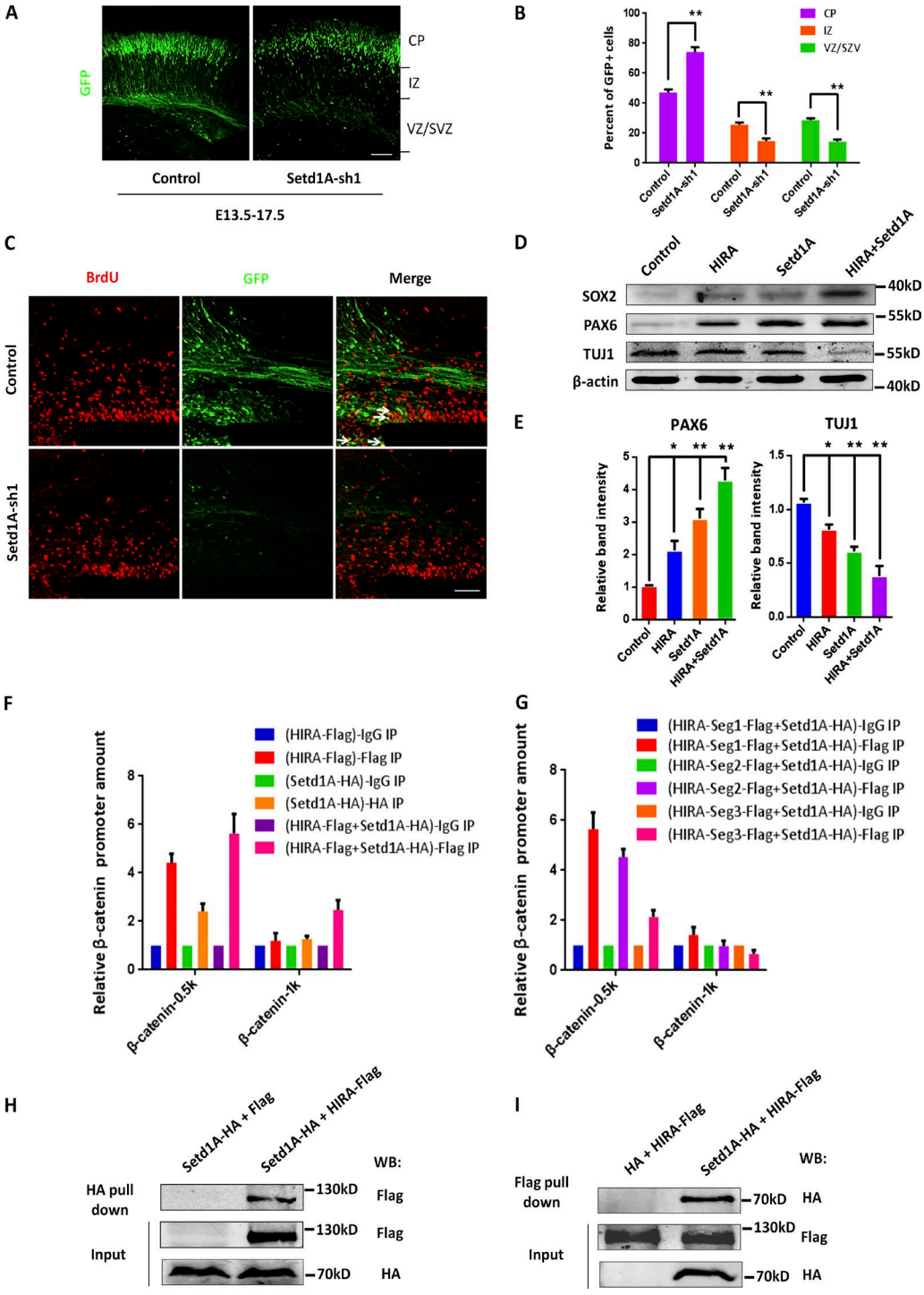

Figure 9. **The H3K4 trimethyltransferase Setd1A can cooperate with HIRA to modulate NPC proliferation.** (A and B) Setd1A knockdown leads to changes in NPC distributions that are similar to that observed after HIRA loss of function. Setd1A-sh1 or control plasmids were electroporated into E13.5 embryonic mouse brains, and embryos were sacrificed at E17.5 for phenotypic analysis. The percentage of GFP-positive cells in each region is analyzed ($n = 3$; mean ± SEM; **, $P < 0.01$; *t* test, two sided). Bar, 50 µm. (C) BrdU and GFP double-positive cells are reduced in Setd1A-sh1 plasmid–electroporated brains. The brains were electroporated at E13.5, and BrdU (100 mg/kg i.p.) was injected into pregnant mice 2 h before the collection of embryos at E17.5. The arrows indicate GFP/BrdU double-positive cells. Bar, 25 µm. (D and E) Setd1A functions together with HIRA to modulate NPC proliferation in vitro. Cultured NPCs were infected with control vector, HIRA vector, Setd1A vector, or HIRA vector together with Setd1A vector, and the protein levels of PAX6, TUJ1, and SOX2 were analyzed using Western blot. The empty control expression vector was used as a control. The bar graph shows the relative band intensity of PAX6 and TUJ1. β-Actin was used as a loading control ($n = 3$; mean ± SEM; *, $P < 0.05$; **, $P < 0.01$; *t* test, two sided). (F) HIRA and Setd1A function together regulate β-catenin levels by binding to the β-catenin promoter. Primary NPCs were infected with control, HIRA overexpression, Setd1A overexpression, and HIRA together with Setd1A overexpression lentiviruses. HIRA and Setd1A binding to the β-catenin promoter was determined using ChIP and real-time PCR ($n = 3$; mean ± SEM). (G) HIRA-Segment 1 and Setd1A collectively modulates β-catenin levels by binding to the β-catenin promoter. Primary NPCs were infected with HIRA-Seg1-Flag, HIRA-Seg2-Flag, or HIRA-Seg3-Flag together with Setd1A-HA co-overexpression lentiviruses, and the anti–Flag

CTGATGATCGAAGTT-3′ (Yang et al., 2011). The shRNAs that targeted β-catenin were β-catenin-sh1, 5′-CTGATATTGACGGGCAGTAT-3′ (Mao et al., 2009), and β-catenin-sh2, 5′-CCCAAGCCTTAGTAAACATAA-3′ (Mao et al., 2009). The shRNAs that targeted Setd1A were Setd1A-sh1, 5′-TGCCCAAACACCCTCTTAATT-3′, and Setd1A-sh2, 5′-CGGCGGTTACTAAGCGCTATT-3′.

Full-length mouse HIRA cDNA and mouse β-catenin cDNA were obtained by PCR and subcloned into the PCDH (CD511B-1; System Biosciences) lentiviral vector to generate Flag-tagged WT expression vectors. Similarly, mouse Setd1A cDNA was amplified by PCR and cloned into an HA-tagged PCDH lentiviral vector.

Three different segments (1–401 aa, 402–703 aa, and 704–1,019 aa) from mouse HIRA cDNA were amplified by PCR and cloned into the PCDH lentiviral vector to generate constructs.

Cell culture and lentivirus packaging

HEK293FT and N2A cells were maintained in DMEM containing 10% FBS, nonessential amino acids, and penicillin/streptomycin in a 37°C incubator with 5% CO_2.

To produce the lentivirus, the plasmid constructs were transfected into 293FT cells by GenEscortI (Nanjing Wisegen Biotechnology). After 8 h, the medium was changed to DMEM containing 10% FBS and nonessential amino acids. The lentivirus was collected at 24, 48, and 72 h after changing the medium. The primary NPCs for immunofluorescence and Western blot were isolated from E12.5 mouse brains and seeded onto 24-well or 6-well plates, which were coated with 10 µg/ml poly-D-Lysine (Sigma-Aldrich) and 10 µg/ml Laminin (Invitrogen) in proliferation medium, which consisted of 50% neural basal medium (Invitrogen), 50% DMEM/F12 (Invitrogen), 10 ng/ml basic FGF (Invitrogen), 10 ng/ml EGF, 2% B27 (without VA), and 1% penicillin/streptomycin. After 12 h, half of the proliferation medium (without penicillin/streptomycin) was changed. Subsequently, the cells were infected with the aforementioned lentiviruses for 8 h, and 2 µg/ml polybrene was added to improve the infection efficiency. After 12 h, the medium was replaced with differentiation medium consisting of low-glucose DMEM (Gibco), 1% FBS (Invitrogen), and 2% B27 (with VA).

Immunostaining

In vitro cell cultures or brain sections were fixed in 4% PFA/PBS for 30 min, washed with PBS three times, and then blocked in 5% BSA/PBS containing 1% Triton X-100 for 1 h. The primary antibody was incubated at 4°C overnight. The next day, sections were washed with PBS three times, and the sections were incubated with secondary antibodies for ∼2 h at RT. For BrdU labeling, sections were treated with 1 M HCl for 10 min at 4°C and 2 M HCl for 10 min at RT and then incubated at 37°C for 20 min. After three washes, the sections were stained with 2 µg/ml DAPI, washed thrice in PBS, and then visualized using the fluorescence-labeled secondary antibodies.

The following primary antibodies were used: mouse anti-HIRA (1:200, 39557; Active Motif), mouse anti-NESTIN (1:200, MAB353; EMD Millipore), mouse anti-SOX2 (1:500; R&D Systems), rabbit anti-TUJ1 (1:1,000, T2200; Sigma-Aldrich), rabbit anti-PAX6 (1:1,000; EMD Millipore), rat anti-BrdU (1:1,000, ab6362; Abcam), rabbit monoclonal anti-Ki67 (1:1,000; Abcam), rabbit anti–phospho-histone H3 (1:500; Cell Signaling Technology), and rabbit anti–total β-catenin (1:1,000, 8480; Cell Signaling Technology).

The secondary antibodies (fluorochromes) used were Cy3 donkey anti–mouse IgG, Cy3 donkey anti–rabbit IgG, Cy5 donkey anti–mouse IgG, and Cy5 donkey anti–rabbit IgG (1:1,000; Jackson ImmunoResearch Laboratories, Inc.).

All confocal images were acquired with the LSM 780 microscope (ZEISS) at RT using a photomultiplier tube detector. The type/magnification/numerical aperture of the objective lenses are Plan-Apochromat 10/0.45, Plan-Apochromat 20/0.8, or Plan-Apochromat 40/1.3 oil; 50% glycerin was applied as imaging medium. The software for image acquisition and processing was ZEN 2010.

Layer definition of the cerebral cortex

There are two main criteria used to identify the boundaries of the cerebral cortex: cell density (visualized with DAPI nuclear staining) and neuronal marker (TUJ1 staining). CP has strong TUJ1 staining and high cell density, the intermediate zone has strong staining of TUJ1 and low cell density, and the VZ/SVZ has faint TUJ1 staining and high cell density (Nguyen et al., 2006).

IUE

E13.5 pregnant ICR mice were deeply anesthetized with 70 mg/kg pentobarbital sodium, and the uterine horns were carefully exposed. Then, 1,500 ng/µl of the overexpression or knockdown plasmid with an enhanced GFP plasmid at a ratio of 3:1 was used. Meanwhile, 0.05% fast green (Sigma-Aldrich) was added as a tracer. Next, using glass capillaries, the mixture of DNA solution (∼1.5 µl/2 µg) was microinjected into the lateral ventricle of the fetal brain. Using platinum electrodes and an electroporator (Manual BTX ECM830) at intervals of 950 ms, five electric pulses of 40 V for 50 ms were performed across the heads of the embryos. After electroporation, the embryos/offspring were sacrificed at E17.5, E19, P2, or P15, and brains were collected for phenotypic analysis. Brains were fixed with 4% PFA at 4°C overnight and then dehydrated in 30% sucrose.

Western blotting

In vitro cultured cells or mouse brain cortical tissue was lysed with RIPA lysis buffer (Solarbio) supplemented with a protease inhibitor cocktail (Sigma-Aldrich) and 10 mM PMSF, and they were centrifuged at 12,000 rpm (4°C) for 10 min to remove cell debris. The concentration of protein was measured using the BCA Protein Assay kit (Thermo Fisher Scientific). Subsequently, equal amounts of protein (in 4× loading buffer) were loaded onto 10% SDS-PAGE gels and transferred to nitrocellulose membranes using the semidry electrophoretic transfer method (Bio-Rad Laboratories). After blocking in 5% skim milk in PBS-T (PBS with 0.05% Tween-20) for 1 h at RT, membranes were incubated with primary antibody at 4°C overnight. To visualize the bands, secondary antibodies were used. Next, the membranes were scanned using the Odyssey Infrared Imaging System. The primary antibodies used for Western blot were mouse anti-HIRA (1:200; 39557; Active Motif), rabbit anti-PAX6 (1:1,000; AB2237; EMD Millipore), mouse anti-TUJ1 (1:1,000; MAB1637; EMD Millipore), rabbit anti-PCNA (1:500; sc7907; Santa Cruz Biotechnology, Inc.), rabbit anti–total β-catenin (1:1,000, 8480; Cell Signaling Technology), rabbit anti-SOX2 (1:1,000; 3579; Cell Signaling Technology), rabbit anti-H3K4me3 (1:1,000; 07–473; EMD Millipore), rabbit anti-Flag (1:1,000; 7425; Sigma-Aldrich), and rabbit anti-IgG (1:1,000; BS0295; Bioss).

antibody was used for immunoprecipitation. Protein binding to the β-catenin promoter was determined through ChIP and real-time PCR (n = 3; mean ± SEM). (H and I) HIRA and Setd1A can be immunoprecipitated together. The immunoprecipitated proteins were probed with anti–HA antibodies to detect HA-Setd1A and anti-Flag antibodies to detect Flag-HIRA. N2A cells were used in this experiment (n = 3). WB, Western blot.

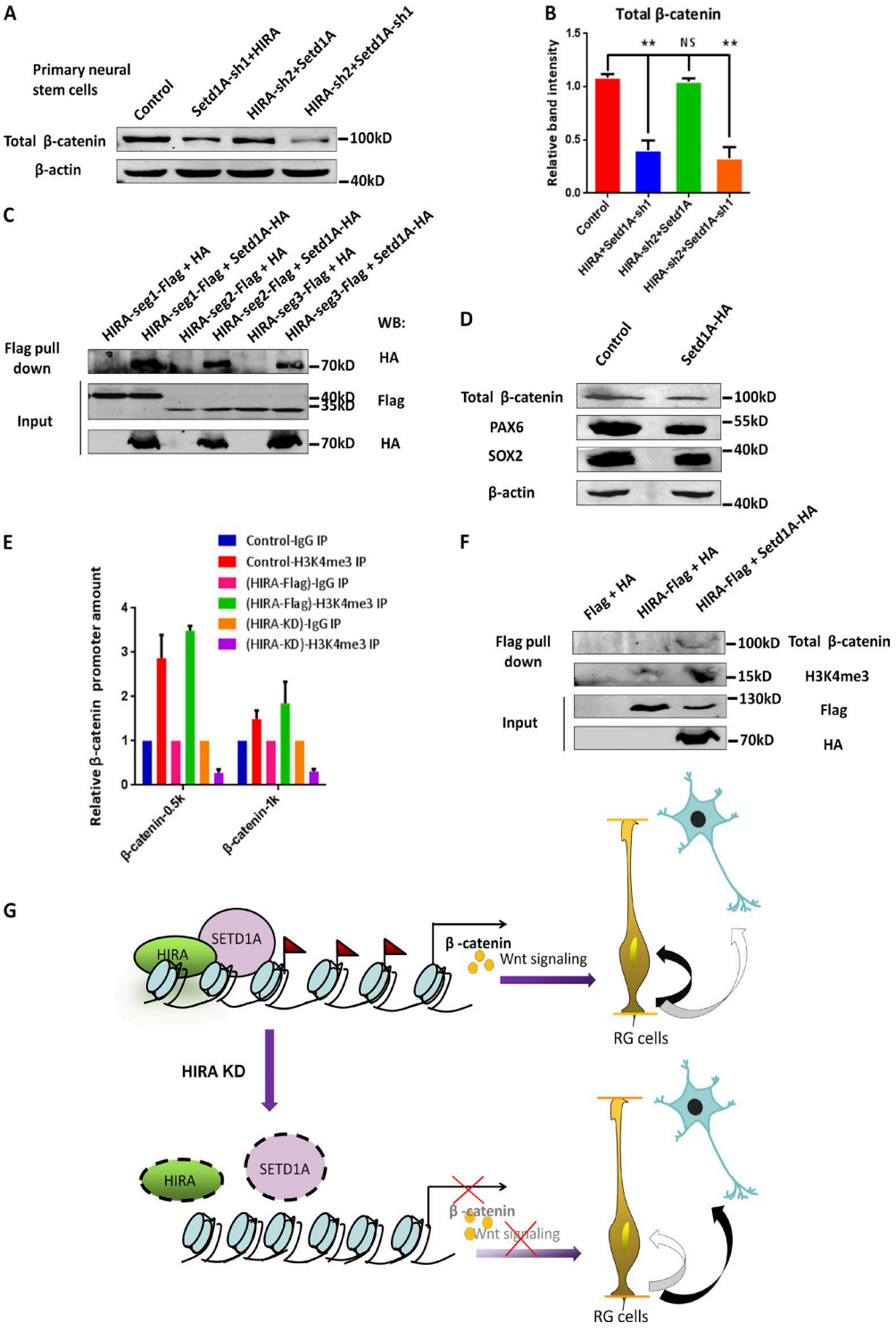

Figure 10. **Setd1A functions downstream of HIRA in regulating β-catenin–mediated NPC proliferation.** (A and B) Western blot analysis of total β-catenin protein levels in NPCs infected with control, Setd1A-sh1 together with HIRA, HIRA-sh2 together with Setd1A, or HIRA-sh2 together with Setd1A-sh1 lentiviruses. The bar graph shows the relative band intensity of total β-catenin. β-Actin was used as a loading control ($n = 3$; mean ± SEM; **, $P < 0.01$; NS, not significant; *t* test, two sided). (C) HIRA segment 1, 2, or 3 all interact with Setd1A. The immunoprecipitated proteins were probed with anti–HA antibodies to detect HA-Setd1A and anti–Flag antibodies to detect Flag-HIRA-segment 1, 2, or 3. N2A cells were used in this experiment ($n = 3$). (D) Western blot analysis of the protein levels of PAX6, SOX2, and β-catenin in cultured NPCs infected with control or Setd1A-sh1 lentiviruses. β-Actin was used as a loading control ($n = 3$). (E) H3K4me3 deposition was increased at the β-catenin locus upon HIRA overexpression and was reduced at the β-catenin locus upon HIRA down-regulation. The anti–H3K4me3 antibody was used for immunoprecipitation (IP). The binding of H3K4me3 to the β-catenin promoter was determined through ChIP and real-time PCR ($n = 3$; mean ± SEM). (F) The expression levels of total β-catenin and H3K4me3 were increased in the anti–Flag antibody immunoprecipitated proteins when HIRA and Setd1A were coexpressed. N2A cells were used in this experiment ($n = 3$). (G) Model of HIRA function in neurogenesis during the embryonic development of the neocortex. HIRA inhibits neurogenesis by recruiting the H3K4 trimethyltransferase Setd1A to the β-catenin promoter. An increase of H3K4me3 expression promotes β-catenin expression and further enhances RGC proliferation. KD, knockdown; RG, retinal ganglion; WB, Western blot.

The secondary antibodies used were 680LT donkey anti–rabbit IgG, 680LT donkey anti–mouse IgG, 800CW donkey anti–rabbit IgG, and 800CW donkey anti–mouse IgG (Odyssey).

Real-time PCR

Total RNA was extracted with TRIzol (15596; Invitrogen), and cDNA was generated from 2 µg RNA using the Fast Quant RT kit (TIANGEN). Real-time PCR was performed using the SYBR Green PCR kit (Takara Bio Inc.) protocol. The following primers were used for real-time PCR: HIRA forward, 5′-CCATGTGTCTGTCTG CACCA-3′, and HIRA reverse, 5′-TCAGGCGACTCAGCCTTATC-3′; β-catenin forward, 5′-ATCACTGAGCCTGCCATCTG-3′, and β-catenin reverse, 5′-GTTGCCACGCCTTCATTC-3′ (Mao et al., 2009); SOX2 forward, 5′-GTGAGCGCCCTGCAGTACAA-3′, and SOX2 reverse, 5′-GCGAGTAGGACATGCTGTAGGTG-3′ (Jiang et al., 2015); CyclinD1 forward, 5′-GCCTACAGCCCTGTTACCTG-3′, and CyclinD1 reverse, 5′-ATTTCATCCCTACCGCTGTG-3′ (Xia et al., 2015); PAX6 forward, 5′-CAGAACAGTCACAGCGGAGT-3′, and PAX6 reverse, 5′-TCCAGCACCTGGACTTTTGC-3′; SOX1 forward, 5′-CCATCTCCAACTCTCAGGGC-3′, and SOX1 reverse, 5′-CCGACTTGACCAGAGATCCG-3′; REST forward, 5′-GTGCGA ACTCACACAGGAGA-3′, and REST reverse, 5′-AAGAGGTTTAGG CCCGTTGT-3′; (Mao et al., 2011). Ngn2 forward, 5′-AGCTCACGA AGATCGAGACG-3′, and Ngn2 reverse, 5′-GTATGGGGACGTGGA GTTGG-3′; YAP forward: 5′-AGGAGAGACTGCGGTTGAAA-3′, and YAP reverse: 5′-CCCAGGAGAAGACACTGCAT-3′ (Xia et al., 2015); Olig2 forward, 5′-GGTGTCTAGTCGCCCATCG-3′, and Olig2 reverse, 5′-AGATGACTTGAAGCCACCGC-3′; Foxg1 forward, 5′-GGCAAGGGCAACTACTGGAT-3′, and Foxg1 reverse, 5′-CGTGGTCCCGTTGTAACTCA-3′; Ki67 forward, 5′-AGCTGC CTGTAGTGTCAAAAA-3′, and Ki67 reverse, 5′-ATCTTGACCTTC CCCATCAGG-3′; Mcm2 forward, 5′-AGAGCTGACCGGCATTTA CC-3′, and Mcm2 reverse, 5′-TTGTGCTTTCCACCTGGGTT-3′; β-actin forward, 5′-GGTGGGAATGGGTCAGAAGG-3′, and β-actin reverse, 5′-AGGAAGAGGATGCGCCAGTG-3′; (Shen et al., 2015b); and Setd1A forward, 5′-CCAACGAGAGTGTGCCCTTT-3′, and Setd1A reverse, 5′-CTGTCCATTGGCCTTTGGTG-3′.

ChIP-qPCR

ChIP was conducted as follows: The in vitro cultured cells were treated with 1% formaldehyde and maintained for 15 min at room temperature to generate the cross-links. Then, to terminate the reaction, 2.5 M glycine was added.

Next, the cells were washed thrice using cold PBS supplemented with a protease inhibitor cocktail and 10 mM PMSF and collected in lysis buffer. Each cell lysate sample was sheared by sonication for 8 min, producing several chromatin fragments with a mean length of 200 bp. The complexes were then incubated with protein A magnetic beads that were previously incubated with 1 µg specific antibody at 4°C overnight. After washing six times with wash buffer (50 mM HEPES-KOH, pH 7.5, 500 mM LiCl, 10 mM EDTA, pH 8.0, 1% Nonidet P40, and 0.7% sodium deoxycholate), the antibody–protein–DNA complex was incubated at 65°C overnight to reverse the covalent bonds. Genomic DNA was extracted from the supernatant using the TIANamp Genomic DNA kit (Tiangen Biotech) for further real-time PCR analysis. The following primers were used for ChIP-qPCR. The following primer sequences for the β-catenin promoter were provided: β-catenin-CDS-Forward, 5′-ACCTGTGCAGCTGGAATTCTC-3′, and β-catenin-CDS-Reverse, 5′-TGACGAAGAGCACAGATGGC-3′; β-catenin-0.5k-Forward, 5′-ACACATAATTTTTGCTGTTAAACT GAT-3′, and β-catenin-0.5k-Reverse, 5′-AGTATGGCATGTTGAAAC ATATGGAG-3′; β-catenin-1k-Forward, 5′-TGTGTGTGTGTGTGT GTGTGTGTGT-3′, and β-catenin-1k-Reverse, 5′-CTTAAAGATATA GTCCCTTCTGATTTTT-3′; and β-catenin-2k-Forward, 5′-TTAAGG CACACTCAGGAGGAAGC-3′, and β-catenin-2k-Reverse, 5′-TGG TTACTGTTAGTCAGTTTGTGGC-3′.

The following primer sequences for the PAX6 promoter were provided: PAX6-0.5k-Forward, 5′-TTGGCCGGGTTTGGG-3′, and PAX6-0.5k-Reverse, 5′-ACCACGAGGGGTCGAAAG-3′; and PAX6-1k-Forward, 5′-AGTGCAGGCTCTAGCCCTC-3′, and PAX6-1k-Reverse, 5′-GATGGTGGGCAAGGAAGGG-3′.

The following primer sequences for the SOX2 promoter were provided: SOX2-0.5k-Forward, 5′-GCACCCTGTTCCAAGTCTCT-3′; SOX2-0.5k-Reverse, 5′-AATCCAACACCATCATAGTCCCC-3′; SOX2-1k-Forward, 5′-ATGCTGAGAAATTCCAGTTAACAA-3′; and SOX2-1k-Reverse, 5′-TGCTTGTTAAAAACGCTTCGC-3′.

Coimmunoprecipitation

A volume of 25 µl Dynabeads Protein A (Thermo Fisher Scientific) that had been incubated with primary antibody (1 µl in PBS containing 0.02% Tween-20) was added into freshly extracted protein samples and incubated at 4°C overnight. The complex including Dynabeads, sample, and antibody was washed thrice and then removed from the supernatant using a magnet. The beads were resuspended with 30 µl 1× loading buffer and heated at 70°C for 10 min. Subsequently, the supernatant was harvested for Western blotting.

Statistical analysis

All images were analyzed with Photoshop CS6 (Adobe). Statistical analyses were performed with Student's *t* test with two-sided analysis (NS, not significant; *, $P < 0.05$; **, $P < 0.01$). Data distribution was assumed to be normal, but this was not formally tested. All data are presented as the mean ± SEM.

All supplemental material studies of neural stem cell proliferation and differentiation were complementary to the main results.

Online supplemental material

Fig. S1 shows real-time PCR detection of HIRA knockdown efficiency. Fig. S2 shows that HIRA knockdown has no effect on NPC apoptosis and that there is little difference in the positioning of GFP-positive cells between the scrambled control shRNA group and the empty control shRNA group. Fig. S3 shows that down-regulation of HIRA promotes cell cycle exit. Fig. S4 shows that HIRA knockdown increases differentiation in vitro. Fig. S5 shows that β-catenin is enriched in isolated NPCs and HIRA knockdown reduces β-catenin in vitro. Fig. S6 shows that Setd1A knockdown reduces proliferation and promotes differentiation of NPCs in utero. Fig. S7 shows protein expression levels for CHIP assays.

Acknowledgments

This work was supported by grants from the National Key Basic Research Program of China (2015CB964500 and 2014CB964903), the National Natural Science Foundation of China (31371477 and 31621004), and K.C. Wong Education Foundation.

The authors declare no competing financial interests.

Author contributions: Y. Li and J. Jiao designed the research; Y. Li performed the research and analyzed the data; and Y. Li and J. Jiao wrote the manuscript.

Submitted: 6 October 2016
Revised: 31 January 2017
Accepted: 19 April 2017

References

Barski, A., S. Cuddapah, K. Cui, T.Y. Roh, D.E. Schones, Z. Wang, G. Wei, I. Chepelev, and K. Zhao. 2007. High-resolution profiling of histone methylations in the human genome. *Cell.* 129:823–837. http://dx.doi.org/10.1016/j.cell.2007.05.009

Bassett, A.S., E.W.C. Chow, P. AbdelMalik, M. Gheorghiu, J. Husted, and R. Weksberg. 2003. The schizophrenia phenotype in 22q11 deletion syndrome. *Am. J. Psychiatry.* 160:1580–1586. http://dx.doi.org/10.1176/appi.ajp.160.9.1580

Berger, S.L. 2007. The complex language of chromatin regulation during transcription. *Nature.* 447:407–412. http://dx.doi.org/10.1038/nature05915

Bernstein, B.E., M. Kamal, K. Lindblad-Toh, S. Bekiranov, D.K. Bailey, D.J. Huebert, S. McMahon, E.K. Karlsson, E.J. Kulbokas III, T.R. Gingeras, et al. 2005. Genomic maps and comparative analysis of histone modifications in human and mouse. *Cell.* 120:169–181. http://dx.doi.org/10.1016/j.cell.2005.01.001

Bird, A. 2007. Perceptions of epigenetics. *Nature.* 447:396–398. http://dx.doi.org/10.1038/nature05913

Clevers, H., K.M. Loh, and R. Nusse. 2014. Stem cell signaling. An integral program for tissue renewal and regeneration: Wnt signaling and stem cell control. *Science.* 346:1248012. http://dx.doi.org/10.1126/science.1248012

Collas, P. 2010. The current state of chromatin immunoprecipitation. *Mol. Biotechnol.* 45:87–100. http://dx.doi.org/10.1007/s12033-009-9239-8

Duque, A., and P. Rakic. 2011. Different effects of bromodeoxyuridine and [3H] thymidine incorporation into DNA on cell proliferation, position, and fate. *J. Neurosci.* 31:15205–15217. http://dx.doi.org/10.1523/JNEUROSCI.3092-11.2011

Dutta, D., S. Ray, P. Home, B. Saha, S. Wang, N. Sheibani, O. Tawfik, N. Cheng, and S. Paul. 2010. Regulation of angiogenesis by histone chaperone HIRA-mediated incorporation of lysine 56-acetylated histone H3.3 at chromatin domains of endothelial genes. *J. Biol. Chem.* 285:41567–41577. http://dx.doi.org/10.1074/jbc.M110.190025

Farrell, M.J., H. Stadt, K.T. Wallis, P. Scambler, R.L. Hixon, R. Wolfe, L. Leatherbury, and M.L. Kirby. 1999. HIRA, a DiGeorge syndrome candidate gene, is required for cardiac outflow tract septation. *Circ. Res.* 84:127–135. http://dx.doi.org/10.1161/01.RES.84.2.127

Felsenfeld, G., and M. Groudine. 2003. Controlling the double helix. *Nature.* 421:448–453. http://dx.doi.org/10.1038/nature01411

Fischle, W., Y. Wang, and C.D. Allis. 2003. Histone and chromatin cross-talk. *Curr. Opin. Cell Biol.* 15:172–183. http://dx.doi.org/10.1016/S0955-0674(03)00013-9

Gregoire, J.-M., L. Fleury, C. Salazar-Cardozo, F. Alby, V. Masson, P.B. Arimondo, and F. Ausseil. 2016. Identification of epigenetic factors regulating the mesenchyme to epithelium transition by RNA interference screening in breast cancer cells. *BMC Cancer.* 16:700. http://dx.doi.org/10.1186/s12885-016-2683-5

Guenther, M.G., S.S. Levine, L.A. Boyer, R. Jaenisch, and R.A. Young. 2007. A chromatin landmark and transcription initiation at most promoters in human cells. *Cell.* 130:77–88. http://dx.doi.org/10.1016/j.cell.2007.05.042

Jiang, X., and J. Nardelli. 2016. Cellular and molecular introduction to brain development. *Neurobiol. Dis.* 92(Pt A):3–17. http://dx.doi.org/10.1016/j.nbd.2015.07.007

Jiang, J., Z. Li, C. Yu, M. Chen, S. Tian, and C. Sun. 2015. MiR-1181 inhibits stem cell-like phenotypes and suppresses SOX2 and STAT3 in human pancreatic cancer. *Cancer Lett.* 356(2, 2 Pt B):962–970. http://dx.doi.org/10.1016/j.canlet.2014.11.007

Leung, J.Y., F.T. Kolligs, R. Wu, Y. Zhai, R. Kuick, S. Hanash, K.R. Cho, and E.R. Fearon. 2002. Activation of AXIN2 expression by beta-catenin-T cell factor. A feedback repressor pathway regulating Wnt signaling. *J. Biol. Chem.* 277:21657–21665. http://dx.doi.org/10.1074/jbc.M200139200

Lin, A., C. Li, Z. Xing, Q. Hu, K. Liang, L. Han, C. Wang, D.H. Hawke, S. Wang, Y. Zhang, et al. 2016. The LINK-A lncRNA activates normoxic HIF1α signalling in triple-negative breast cancer. *Nat. Cell Biol.* 18:213–224. http://dx.doi.org/10.1038/ncb3295

Lorain, S., S. Demczuk, V. Lamour, S. Toth, A. Aurias, B.A. Roe, and M. Lipinski. 1996. Structural organization of the WD repeat protein-encoding gene HIRA in the DiGeorge syndrome critical region of human chromosome 22. *Genome Res.* 6:43–50. http://dx.doi.org/10.1101/gr.6.1.43

Majumder, A., K.M. Syed, S. Joseph, P.J. Scambler, and D. Dutta. 2015. Histone chaperone HIRA in regulation of transcription factor RUNX1. *J. Biol. Chem.* 290:13053–13063. http://dx.doi.org/10.1074/jbc.M114.615492

Mao, C.A., W.W. Tsai, J.H. Cho, P. Pan, M.C. Barton, and W.H. Klein. 2011. Neuronal transcriptional repressor REST suppresses an Atoh7-independent program for initiating retinal ganglion cell development. *Dev. Biol.* 349:90–99. http://dx.doi.org/10.1016/j.ydbio.2010.10.008

Mao, Y., X. Ge, C.L. Frank, J.M. Madison, A.N. Koehler, M.K. Doud, C. Tassa, E.M. Berry, T. Soda, K.K. Singh, et al. 2009. Disrupted in schizophrenia 1 regulates neuronal progenitor proliferation via modulation of GSK3beta/beta-catenin signaling. *Cell.* 136:1017–1031. http://dx.doi.org/10.1016/j.cell.2008.12.044

Maze, I., W. Wenderski, K.M. Noh, R.C. Bagot, N. Tzavaras, I. Purushothaman, S.J. Elsässer, Y. Guo, C. Ionete, Y.L. Hurd, et al. 2015. Critical role of histone turnover in neuronal transcription and plasticity. *Neuron.* 87:77–94. http://dx.doi.org/10.1016/j.neuron.2015.06.014

McConnell, S.K. 1995. Constructing the cerebral cortex: Neurogenesis and fate determination. *Neuron.* 15:761–768. http://dx.doi.org/10.1016/0896-6273(95)90168-X

McDonald-McGinn, D.M., and K.E. Sullivan. 2011. Chromosome 22q11.2 deletion syndrome (DiGeorge syndrome/velocardiofacial syndrome). *Medicine (Baltimore).* 90:1–18. http://dx.doi.org/10.1097/MD.0b013e3182060469

Nashun, B., P.W. Hill, S.A. Smallwood, G. Dharmalingam, R. Amouroux, S.J. Clark, V. Sharma, E. Ndjetehe, P. Pelczar, R.J. Festenstein, et al. 2015. Continuous histone replacement by hira is essential for normal transcriptional regulation and de novo DNA methylation during mouse oogenesis. *Mol. Cell.* 60:611–625. http://dx.doi.org/10.1016/j.molcel.2015.10.010

Nguyen, L., A. Besson, J.I. Heng, C. Schuurmans, L. Teboul, C. Parras, A. Philpott, J.M. Roberts, and F. Guillemot. 2006. p27kip1 independently promotes neuronal differentiation and migration in the cerebral cortex. *Genes Dev.* 20:1511–1524. http://dx.doi.org/10.1101/gad.377106

Niehrs, C. 2012. The complex world of WNT receptor signalling. *Nat. Rev. Mol. Cell Biol.* 13:767–779. http://dx.doi.org/10.1038/nrm3470

Qian, X., Q. Shen, S.K. Goderie, W. He, A. Capela, A.A. Davis, and S. Temple. 2000. Timing of CNS cell generation: a programmed sequence of neuron and glial cell production from isolated murine cortical stem cells. *Neuron.* 28:69–80. http://dx.doi.org/10.1016/S0896-6273(00)00086-6

Reik, W. 2007. Stability and flexibility of epigenetic gene regulation in mammalian development. *Nature.* 447:425–432. http://dx.doi.org/10.1038/nature05918

Ross, C.A., R.L. Margolis, S.A.J. Reading, M. Pletnikov, and J.T. Coyle. 2006. Neurobiology of schizophrenia. *Neuron.* 52:139–153. http://dx.doi.org/10.1016/j.neuron.2006.09.015

Shen, E.Y., T.H. Ahern, I. Cheung, J. Straubhaar, A. Dincer, I. Houston, G.J. de Vries, S. Akbarian, and N.G. Forger. 2015a. Epigenetics and sex differences in the brain: A genome-wide comparison of histone-3 lysine-4 trimethylation (H3K4me3) in male and female mice. *Exp. Neurol.* 268:21–29. http://dx.doi.org/10.1016/j.expneurol.2014.08.006

Shen, T., F. Ji, Z. Yuan, and J. Jiao. 2015b. CHD2 is required for embryonic neurogenesis in the developing cerebral cortex. *Stem Cells.* 33:1794–1806. http://dx.doi.org/10.1002/stem.2001

Singh, T., M.I. Kurki, D. Curtis, S.M. Purcell, L. Crooks, J. McRae, J. Suvisaari, H. Chheda, D. Blackwood, G. Breen, et al.; UK10 K Consortium. 2016. Rare loss-of-function variants in SETD1A are associated with schizophrenia and developmental disorders. *Nat. Neurosci.* 19:571–577. http://dx.doi.org/10.1038/nn.4267

Stratton, M.S., and T.A. McKinsey. 2016. Epigenetic regulation of cardiac fibrosis. *J. Mol. Cell. Cardiol.* 92:206–213. http://dx.doi.org/10.1016/j.yjmcc.2016.02.011

Szenker, E., N. Lacoste, and G. Almouzni. 2012. A developmental requirement for HIRA-dependent H3.3 deposition revealed at gastrulation in Xenopus. *Cell Reports.* 1:730–740. http://dx.doi.org/10.1016/j.celrep.2012.05.006

Tajima, K., T. Yae, S. Javaid, O. Tam, V. Comaills, R. Morris, B.S. Wittner, M. Liu, A. Engstrom, F. Takahashi, et al. 2015. SETD1A modulates cell cycle progression through a miRNA network that regulates p53 target genes. *Nat. Commun.* 6:8257. http://dx.doi.org/10.1038/ncomms9257

Takata, A., B. Xu, I. Ionita-Laza, J.L. Roos, J.A. Gogos, and M. Karayiorgou. 2014. Loss-of-function variants in schizophrenia risk and SETD1A as a candidate susceptibility gene. *Neuron.* 82:773–780. http://dx.doi.org/10.1016/j.neuron.2014.04.043

Wiese, C., A. Rolletschek, G. Kania, P. Blyszczuk, K.V. Tarasov, Y. Tarasova, R.P. Wersto, K.R. Boheler, and A.M. Wobus. 2004. Nestin expression--a property of multi-lineage progenitor cells? *Cell. Mol. Life Sci.* 61:2510–2522. http://dx.doi.org/10.1007/s00018-004-4144-6

Wilming, L.G., C.A.S. Snoeren, A. van Rijswijk, F. Grosveld, and C. Meijers. 1997. The murine homologue of HIRA, a DiGeorge syndrome candidate gene, is expressed in embryonic structures affected in human CATCH22 patients. *Hum. Mol. Genet.* 6:247–258. http://dx.doi.org/10.1093/hmg/6.2.247

Xia, W., Y. Liu, and J. Jiao. 2015. GRM7 regulates embryonic neurogenesis via CREB and YAP. *Stem Cell Rep.* 4:795–810. http://dx.doi.org/10.1016/j.stemcr.2015.03.004

Xu, D., F. Zhang, Y. Wang, Y. Sun, and Z. Xu. 2014. Microcephaly-associated protein WDR62 regulates neurogenesis through JNK1 in the developing neocortex. *Cell Rep.* 6:104–116. http://dx.doi.org/10.1016/j.celrep.2013.12.016

Yang, J.H., Y. Song, J.H. Seol, J.Y. Park, Y.J. Yang, J.W. Han, H.D. Youn, and E.J. Cho. 2011. Myogenic transcriptional activation of MyoD mediated by replication-independent histone deposition. *Proc. Natl. Acad. Sci. USA.* 108:85–90. http://dx.doi.org/10.1073/pnas.1009830108

Yao, B., K.M. Christian, C. He, P. Jin, G.L. Ming, and H. Song. 2016. Epigenetic mechanisms in neurogenesis. *Nat. Rev. Neurosci.* 17:537–549. http://dx.doi.org/10.1038/nrn.2016.70

Zechner, D., Y. Fujita, J. Hülsken, T. Müller, I. Walther, M.M. Taketo, E.B. Crenshaw III, W. Birchmeier, and C. Birchmeier. 2003. β-Catenin signals regulate cell growth and the balance between progenitor cell expansion and differentiation in the nervous system. *Dev. Biol.* 258:406–418. http://dx.doi.org/10.1016/S0012-1606(03)00123-4

Zinkstok, J., and T. van Amelsvoort. 2005. Neuropsychological profile and neuroimaging in patients with 22Q11.2 deletion syndrome: A review. *Child Neuropsychol.* 11:21–37. http://dx.doi.org/10.1080/09297040590911194